The Journal of Chemical Physics

Reversible target-binding kinetics of multiple impatient particles

Cite as: J. Chem. Phys. **156**, 084107 (2022); https://doi.org/10.1063/5.0083849
Submitted: 30 December 2021 • Accepted: 04 February 2022 • Accepted Manuscript Online: 04 February 2022 • Published Online: 22 February 2022

Denis S. Grebenkov and Aanjaneya Kumar

The Journal of Chemical Physics ARTICLE scitation.org/journal/jcp

Reversible target-binding kinetics of multiple impatient particles

Cite as: J. Chem. Phys. 156, 084107 (2022); doi: 10.1063/5.0083849
Submitted: 30 December 2021 • Accepted: 4 February 2022 •
Published Online: 22 February 2022

Denis S. Grebenkov[1,a] and Aanjaneya Kumar[2,b]

AFFILIATIONS

[1] Laboratoire de Physique de la Matière Condensée (UMR 7643), CNRS–Ecole Polytechnique, IP Paris, 91120 Palaiseau, France
[2] Department of Physics, Indian Institute of Science Education and Research, Dr. Homi Bhabha Road, Pune 411008, India

[a] **Author to whom correspondence should be addressed:** denis.grebenkov@polytechnique.edu
[b] **Electronic mail:** kumar.aanjaneya@students.iiserpune.ac.in

ABSTRACT

Certain biochemical reactions can only be triggered after binding a sufficient number of particles to a specific target region such as an enzyme or a protein sensor. We investigate the distribution of the reaction time, i.e., the first instance when all independently diffusing particles are bound to the target. When each particle binds irreversibly, this is equivalent to the first-passage time of the slowest (last) particle. In turn, reversible binding to the target renders the problem much more challenging and drastically changes the distribution of the reaction time. We derive the exact solution of this problem and investigate the short-time and long-time asymptotic behaviors of the reaction time probability density. We also analyze how the mean reaction time depends on the unbinding rate and the number of particles. Our exact and asymptotic solutions are compared to Monte Carlo simulations.

I. INTRODUCTION

Diffusion-controlled reactions play an important role in many chemical and biological processes. In a typical scenario, particles diffuse in a confining domain toward a specific target region to react or to trigger a biological event.[1–9] Various aspects of such diffusive search processes have been investigated, with the particular emphasis on first-passage times (FPTs) that characterize how fast a single particle finds a single target. The distribution of the first-passage time τ is usually described by the survival probability, $S(t) = \mathbb{P}\{\tau > t\}$, or, equivalently, by the probability density function $H(t) = -dS(t)/dt$. The distribution and, particularly, the mean value $\langle\tau\rangle$ and the associate reaction rate have been thoroughly analyzed.[10–41]

As the diffusive search is typically long, many independent searchers are generally involved to speed up this process. In this setting, the arrival of the *fastest* particle among N particles can trigger the reaction. If $\tau_1, \ldots, \tau_N$ denote the FPTs of these particles, the fastest first-passage time (fFPT) is $\mathcal{T}^0_{1,N} = \min\{\tau_1, \ldots, \tau_N\}$. As the particles search independently, the distribution of the fFPT is simply given as

$$\mathbb{P}\{\mathcal{T}^0_{1,N} > t\} = \mathbb{P}\{\tau_1 > t\} \ldots \mathbb{P}\{\tau_N > t\} = [S(t)]^N. \tag{1}$$

Similarly, the first-passage time $\mathcal{T}^0_{K,N}$ of the Kth fastest particle to arrive onto the target is governed by the following law:

$$\mathbb{P}\{\mathcal{T}^0_{K,N} > t\} = \sum_{j=0}^{K-1} \binom{N}{j} [S(t)]^{N-j} [1 - S(t)]^j, \tag{2}$$

where $\binom{N}{j}$ is the binomial coefficient. The associated probability density follows immediately,

$$H^0_{K,N}(t) = -\frac{d\mathbb{P}\{\mathcal{T}^0_{K,N} > t\}}{dt} = K\binom{N}{K}[S(t)]^{N-K}[1 - S(t)]^{K-1} H(t). \tag{3}$$

While these expressions fully characterize the random variable $\mathcal{T}^0_{K,N}$, finding the large-N asymptotic behavior of its moments, $\langle[\mathcal{T}^0_{K,N}]^m\rangle$, is a difficult problem. More generally, random variables $\mathcal{T}^0_{K,N}$ present an example of extreme value statistics.[42]

This problem was first studied by Weiss *et al.* who showed by analyzing the exact form of $S(t)$ for one-dimensional diffusion on an interval that the mean $\langle\mathcal{T}^0_{K,N}\rangle$ decreases logarithmically

slowly with N: $\langle \mathcal{T}^0_{K,N} \rangle \propto 1/\ln N$ as $N \to \infty$.[43] They also briefly considered higher-order moments and argued the universality of the logarithmic decay for other diffusive processes. This seminal work was further extended by several authors.[44–51] For instance, Basnayake *et al.* and Lawley and Madrid gave rigorous mathematical proofs for the asymptotic behavior of these moments[44–46] (see also Appendix A 1 for new results concerning the behavior of the mean of the *slowest* FPT $\mathcal{T}^0_{N,N}$). In addition, Lawley found the parameters of the asymptotic Gumbel distribution of $\mathcal{T}^0_{1,N}$ for a large class of diffusion processes.[47] Moreover, this result was extended to the Kth fastest FPT $\mathcal{T}^0_{K,N}$, and the asymptotic form of the joint distribution of $\{\mathcal{T}^0_{1,N}, \ldots, \mathcal{T}^0_{K,N}\}$ was derived. The logarithmic scaling of the mean fFPT was evoked to rationalize the redundancy in the number of searchers in some biological systems, such as the large number of sperm cells.[49,50] We stress, however, that a logarithmic speed up of the search process is too costly from a practical point of view; for instance, a ten-fold reduction of the mean time would require more than twenty thousands of particles. Note that if the starting positions of N particles are uniformly distributed in the domain, the logarithmic decay is replaced by a much faster power law decay: $\langle \mathcal{T}^0_{1,N} \rangle \propto 1/N$ for partially reactive targets and $\langle \mathcal{T}^0_{1,N} \rangle \propto 1/N^2$ for perfectly reactive targets.[48] More generally, the power law decay $1/N$ was shown to emerge as a transient regime of moderately large N if the target is small or if finding the target requires escaping a potential well.[51] Moreover, as the mean value is not always the relevant time scale of the process,[30,33,52] evolutionary optimization of diffusive search does not necessarily aim at reducing the mean value of the fFPT.

In the above discussion, each particle that arrived onto the target was supposed to remain on it forever. In particular, the number $\mathcal{N}(t)$ of particles bound to the target at time t is a non-decreasing stochastic process that increases by 1 at the arrival of each new particle. As a consequence, the Kth fastest FPT $\mathcal{T}^0_{K,N}$ is equal to the first instance $\mathcal{T}_{K,N} = \inf\{t > 0 \ : \ \mathcal{N}(t) = K\}$ when K particles among N are bound to the target. In many chemical and biological settings, however, binding to the target is a *reversible* process, i.e., each particle remains on the target for some waiting time, unbinds from it, and resumes its bulk diffusion. The waiting time is usually considered to be an independent random variable obeying an exponential law with the rate $k_{\rm off}$. As each unbinding event diminishes $\mathcal{N}(t)$ by 1, the number of bound particles is no longer a non-decreasing process (Fig. 1). Even though the dynamics of all particles is Markovian (i.e., their positions and states at time t fully determine the probabilities of their positions and states in the future), the number $\mathcal{N}(t)$ of bound particles is a non-Markovian process. The reversible binding does not affect the statistics of the first instance $\mathcal{T}_{1,N}$ when one particle (the fastest one) is bound to the target, i.e., Eq. (1) governs the probability law for $\mathcal{T}_{1,N} = \mathcal{T}^0_{1,N}$. In contrast, the first instance $\mathcal{T}_{K,N}$ for K particles to be bound to the target is no longer equal to the Kth fastest FPT $\mathcal{T}^0_{K,N}$. Indeed, before the binding of the Kth particle, some of the previously bound particles can unbind, and thus, $\mathcal{T}_{K,N} \geq \mathcal{T}^0_{K,N}$ (the superscript 0 highlights that the first-passage times $\mathcal{T}^0_{K,N}$ correspond to irreversible binding with $k_{\rm off} = 0$). Even though the particles are independent, random waiting times spent by these particles on the target render the characterization of the reaction times $\mathcal{T}_{K,N}$ much more challenging than that of $\mathcal{T}^0_{K,N}$. As reversible binding allows some particles to leave the target before the arrival of the others, they were termed *impatient*.[53] In Ref. 53, the problem of two impatient particles diffusing on an interval was mapped onto intermittent diffusion on a square. Solving the latter problem, the mean $\langle \mathcal{T}_{2,2} \rangle$ was obtained, and the effect of reversible binding was analyzed. Even this basic case with two particles required sophisticated analysis.

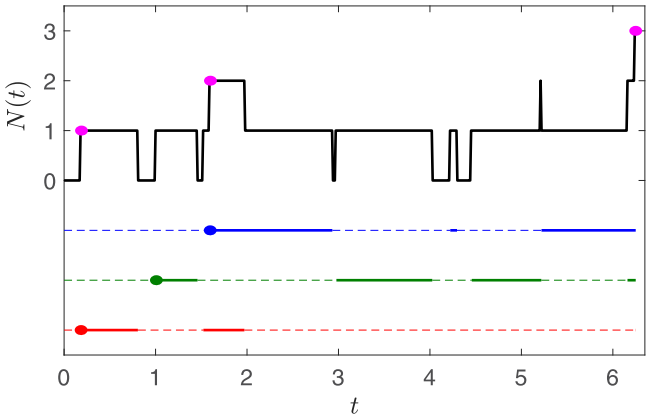

FIG. 1. Illustration of a simulated process $\mathcal{N}(t)$ that counts the number of bound particles at time t with $N = 3$. Three filled circles indicate the first-crossing times $\mathcal{T}_{K,N}$ for $K = 1, 2, 3$. On the bottom, there is a schematic representation of the state of each of three particles: free state (thin dashed line) vs bound state (thick solid line). Three filled circles indicate the first-passage times $\mathcal{T}^0_{K,N}$ for the first, second, and third particles (in the order of arrival). While $\mathcal{T}_{1,N} = \mathcal{T}^0_{1,N}$, unbinding events imply that $\mathcal{T}_{K,N} \geq \mathcal{T}^0_{K,N}$ for any $K > 1$.

Lawley and Madrid proposed a remarkable approximation to the general problem.[54] Assuming that the first-binding time and the rebinding time (i.e., the random time between unbinding of a particle from the target and its next rebinding) can be approximated by an exponential random variable with some rate ν, the number $\mathcal{N}(t)$ can be modeled by a Markovian birth–death process $\overline{\mathcal{N}}(t)$ between $N + 1$ states of $0, 1, 2, \ldots, N$ bound particles,

$$0 \underset{k_{\rm off}}{\overset{N\nu}{\rightleftarrows}} 1 \underset{2k_{\rm off}}{\overset{(N-1)\nu}{\rightleftarrows}} 2 \quad \cdots \quad N-1 \underset{Nk_{\rm off}}{\overset{\nu}{\rightleftarrows}} N \tag{4}$$

(here and throughout the text, bar denotes the quantities corresponding to the Lawley–Madrid approximation). Introducing an $(N + 1) \times (N + 1)$-dimensional matrix W with zero elements except for

$$W_{i,i+1} = ik_{\rm off}, \quad W_{i+1,i} = (N + 1 - i)\nu \quad (i = 1, 2, \ldots, N)$$

and $W_{i,i}$ that are chosen so that W has zero column sums, the distribution of the first-crossing time $\overline{\mathcal{T}}_{K,N} = \inf\{t > 0 \ : \ \overline{\mathcal{N}}(t) = K\}$ can be written as[54]

$$\mathbb{P}\{\overline{\mathcal{T}}_{K,N} > t\} = \sum_{j=1}^{K} \left[\exp(W^{(K)}t)\right]_{j,1}, \tag{5}$$

where $W^{(K)}$ is the $K \times K$ matrix obtained by retaining the first K columns and K rows from W and discarding everything else. Here, the initial state was assumed to be 0, i.e., no bound particles. In other words, the distribution is expressed in terms of the

matrix exponential of $W^{(K)}$. The probability density of $\overline{\mathcal{T}}_{K,N}$ is even simpler,

$$\overline{H}_{K,N}(t) = \nu(N-K+1)\left[\exp\left(W^{(K)}t\right)\right]_{K,1}. \tag{6}$$

Finally, the mean time is fully explicit,

$$\langle\overline{\mathcal{T}}_{K,N}\rangle = \frac{1}{\nu}\sum_{m=1}^{K}\left(\frac{1}{b_m} + \sum_{j=m+1}^{K}\frac{(k_{\rm off}/\nu)^{j-m}}{b_j}\prod_{i=m}^{j-1}\frac{d_i}{b_i}\right) \tag{7}$$

with $b_m = N-K+m$ and $d_m = K-m$. Lawley and Madrid proved that $\overline{\mathcal{N}}(t)$ and $\overline{\mathcal{T}}_{K,N}$ are universal bounds to $\mathcal{N}(t)$ and $\mathcal{T}_{K,N}$,

$$\mathcal{N}(t) \geq \overline{\mathcal{N}}(t) \quad \text{for all } t, \qquad \mathcal{T}_{K,N} \leq \overline{\mathcal{T}}_{K,N} \quad \text{for all } K, \tag{8}$$

which actually means that

$$\mathbb{P}\{\mathcal{N}(t) > K\} \geq \mathbb{P}\{\overline{\mathcal{N}}(t) > K\}, \tag{9}$$

$$\mathbb{P}\{\mathcal{T}_{K,N} > t\} \leq \mathbb{P}\{\overline{\mathcal{T}}_{K,N} > t\}. \tag{10}$$

Moreover, when the target region is getting smaller and smaller, these bounds become more and more accurate.

The Lawley–Madrid approximation (LMA) opens a way to investigate in detail the role of reversible binding onto the statistics of sophisticated biochemical processes involving the arrival of several molecules onto the target region. The prominent example is the signaling process between neurons when the fusion of a neurotransmitters vesicle with the presynaptic bouton membrane is triggered by the arrival of five calcium ions onto the sensor protein.[2,52,55–59] It was recently shown by extensive simulations that unbinding events considerably affect the fusion probability.[52]

Despite numerous advantages of the LMA, it relies on a rough assumption that both first-binding and rebinding times can be modeled by an exponential random variable. However, the probability density of the rebinding time is, in general, more sophisticated; for instance, in the case of a spherical target, it diverges at short times as $H(t) \propto t^{-1/2}$ (see Appendix B), in sharp contrast to the assumed exponential density $\nu e^{-\nu t}$ that behaves as $\nu + O(t)$ as $t \to 0$. This observation suggests that the LMA does not correctly capture the short-time behavior that can be relevant for some applications. In this paper, we undertake a systematic study of the problem of impatient particles in the case $K = N$. Using the renewal approach, we derive the exact solution for this problem. We deduce the short-time and long-time behavior of this solution and compare it with the LMA predictions and with Monte Carlo simulations. The short-time asymptotic analysis is also extended to arbitrary K. We show that the LMA captures the qualitative behavior of the reaction time distribution at moderate and long times. However, the LMA overestimates the mean reaction time and the decay time and fails at short times. From the practical point of view, the LMA can thus be used for qualitative estimations, but further improvements are necessary for getting more accurate results.

This paper is organized as follows. In Sec. II, we start with the mathematical model of impatient particles, derive the exact form of the probability density of the reaction time $\mathcal{T}_{N,N}$, and analyze its short-time and long-time asymptotic behavior. We also obtain the mean reaction time $\langle\mathcal{T}_{N,N}\rangle$ and the decay time T_N of the exponential decrease of the probability density at long times. We illustrate the obtained results for a relevant example of restricted diffusion toward a spherical target. Section III is devoted to a systematic comparison of the exact solution with two reference solutions: the irreversible binding case and the LMA. In Sec. IV, we summarize our findings, discuss eventual applications, and provide final remarks and perspectives. Technical details of the asymptotic analysis, the summary of formulas for restricted diffusion between two concentric spheres, the numerical implementation of the exact solution, and the description of Monte Carlo simulations are given in Appendixes A–D, respectively.

II. MAIN RESULTS

A. Mathematical model of impatient particles

We consider N independent indistinguishable point-like particles diffusing with diffusion coefficient D inside a bounded Euclidean domain $\Omega \subset \mathbb{R}^d$. The boundary $\partial\Omega$ of Ω is reflecting everywhere, except for a partially reactive target region Γ. After hitting the target, a particle can bind to it with some probability controlled by the reactivity κ.[30,37,48,60–73] This binding is reversible, i.e., the bound particle stays on the target for an independent random waiting time distributed according to the exponential law with the rate $k_{\rm off}$. After unbinding from the target, the particle resumes its bulk diffusion from a random uniformly distributed location on the target boundary until the next time it binds to the target. We are interested in computing the probability density $H_N(t|\boldsymbol{x}_0) = H_{N,N}(t|\boldsymbol{x}_0)$ of the first instance $\mathcal{T}_N = \mathcal{T}_{N,N}$ when all of the N particles are bound to the target [i.e., when the process $\mathcal{N}(t)$ crosses the level N for the first time]. As the arrival of N particles to the target is supposed to trigger some reaction event, the first-crossing time $\mathcal{T}_N$ is called the *reaction time*. For simplicity, we assume that all the particles are initially free (not bound to the target) and start from the same initial position $\boldsymbol{x}_0 \in \Omega$. These starting assumptions can be easily relaxed.

B. Exact solution

To proceed, we introduce the probability $\mathcal{P}_t(n|m)$ that starting from m particles bound to the target at time 0, there are n particles bound to the target at time t. This probability is hard to compute, in general, due to unbinding events. However, there are two particular cases for which $\mathcal{P}_t(n|m)$ can be expressed in terms of a single particle dynamics. Let $P(t|\boldsymbol{x}_0)$ denote the occupancy probability that an initially free particle that started from a point $\boldsymbol{x}_0$ is bound to the target at time t. Since all particles are independent, the probability of finding m bound particles on the target at time t is

$$\mathcal{P}_t(m|0) = \binom{N}{m}[P(t|\boldsymbol{x}_0)]^m[1-P(t|\boldsymbol{x}_0)]^{N-m}, \tag{11}$$

where we have chosen the initial condition that all particles are initially free. Similarly, if $Q(t)$ denotes the probability that, starting from the bound state at time 0, the particle is bound to the target at time t, then

$$\mathcal{P}_t(m|N) = \binom{N}{m}[Q(t)]^m[1-Q(t)]^{N-m}. \tag{12}$$

The probability density of the reaction time $\mathcal{T}_N$ can then be obtained from a standard renewal equation,

$$\mathcal{P}_t(N|0) = \int_0^t dt'\, H_N(t')\, \mathcal{P}_{t-t'}(N|N). \tag{13}$$

Switching to Laplace space allows us to get

$$\widetilde{H}_N(p|\boldsymbol{x}_0) = \frac{\mathcal{L}\{[P(t|\boldsymbol{x}_0)]^N\}}{\mathcal{L}\{[Q(t)]^N\}}, \tag{14}$$

where both $\mathcal{L}$ and tilde denote the Laplace transform, e.g.,

$$\widetilde{f}(p) = \mathcal{L}[f(t)] = \int_0^\infty dt\, e^{-pt} f(t).$$

The inversion of the Laplace transform gives the probability density in the time domain,

$$H_N(t|\boldsymbol{x}_0) = \mathcal{L}^{-1}\left\{\frac{\mathcal{L}\{[P(t|\boldsymbol{x}_0)]^N\}}{\mathcal{L}\{[Q(t)]^N\}}\right\}. \tag{15}$$

The last step consists in relating the probabilities $P(t|\boldsymbol{x}_0)$ and $Q(t)$ to the first-passage time statistics of a single particle. This can be done in a standard way by summing contributions according to the number of unbinding events (see, e.g., Ref. 52). For instance, one finds

$$Q(t) = \Psi(t) + \int_0^t dt_1\, \psi(t_1) \int_{t_1}^t dt_1'\, H(t_1' - t_1)\, \Psi(t - t_1') + \cdots,$$

where $\Psi(t) = e^{-k_{\rm off}t}$ is the probability of staying in the bound state up to time t, $\psi(t) = -d\Psi(t)/dt = k_{\rm off}e^{-k_{\rm off}t}$ is the probability density of the associated waiting time, and $H(t)$ is the probability density of the rebinding time. The first term in the above equation is the contribution without unbinding. In the second term, the particle unbinds at time t_1, diffuses in the bulk until the next rebinding at time t_1', and remains bound until time t. The third and next terms correspond to 2, 3, etc., unbinding events. In the Laplace domain, one simply gets

$$\widetilde{Q}(p) = \widetilde{\Psi}(p) + \widetilde{\psi}(p)\widetilde{H}(p)\widetilde{\Psi}(p) + \cdots = \frac{\widetilde{\Psi}(p)}{1 - \widetilde{\psi}(p)\widetilde{H}(p)}$$
$$= \frac{1}{p + k_{\rm off}(1 - \widetilde{H}(p))}. \tag{16}$$

In turn, the occupancy probability $P(t|\boldsymbol{x}_0)$ includes an additional step of the first-passage to the target that yields

$$\widetilde{P}(p|\boldsymbol{x}_0) = \widetilde{H}(p|\boldsymbol{x}_0)\, \widetilde{Q}(p) \tag{17}$$
$$= \frac{\widetilde{H}(p|\boldsymbol{x}_0)}{p + k_{\rm off}(1 - \widetilde{H}(p))}, \tag{18}$$

where $\widetilde{H}(p|\boldsymbol{x}_0)$ is the Laplace transform of the probability density $H(t|\boldsymbol{x}_0)$ of the first-passage time to the target when the particle started from a point $\boldsymbol{x}_0$. Note that as the particle is released after unbinding from a uniformly distributed point on the target boundary Γ, one also gets

$$H(t) = \frac{1}{|\Gamma|}\int_\Gamma d\boldsymbol{x}_0\, H(t|\boldsymbol{x}_0), \tag{19}$$

where $|\Gamma|$ is the Lebesgue measure of Γ (e.g., the area of Γ in the three-dimensional case). In this way, both probabilities $P(t|\boldsymbol{x}_0)$ and $Q(t)$ are expressed in terms of the first-passage time probability density $H(t|\boldsymbol{x}_0)$ for a single particle. In the case $N = 1$, a comparison of Eqs. (14) and (17) immediately yields that $H_1(t|\boldsymbol{x}_0) = H(t|\boldsymbol{x}_0)$, as expected.

C. Spectral decompositions

As we deal with restricted diffusion in a bounded domain, the probabilities $P(t|\boldsymbol{x}_0)$ and $Q(t)$ can be formally deduced from their Laplace transforms by applying the residue theorem. Let $\{p_n\}$ be the poles of $\widetilde{P}(p|\boldsymbol{x}_0)$ that lie on the *negative* real axis: $0 = p_0 > p_1 \geq p_2 \geq \searrow -\infty$. According to Eq. (18), these poles satisfy the following equation:

$$p_n + k_{\rm off}(1 - \widetilde{H}(p_n)) = 0. \tag{20}$$

Note that since the poles of $\widetilde{H}(p|\boldsymbol{x}_0)$ and $\widetilde{H}(p)$ are the same, they cancel each other in Eq. (18) and thus are not included in the set of poles of $\widetilde{P}(p|\boldsymbol{x}_0)$. If all the poles are simple, the inverse Laplace transform yields

$$P(t|\boldsymbol{x}_0) = P_\infty + \sum_{n=1}^\infty v_n(\boldsymbol{x}_0)\, e^{p_n t}, \tag{21}$$

where $v_n(\boldsymbol{x}_0)$ is the residue of $\widetilde{P}(p|\boldsymbol{x}_0)$ evaluated at the pole p_n. The steady-state limit P_∞ corresponds to the pole at 0, which can be obtained by using the Taylor expansion

$$\widetilde{H}(p|\boldsymbol{x}_0) = \langle e^{-p\tau}\rangle_{\boldsymbol{x}_0} = 1 - p\langle\tau\rangle_{\boldsymbol{x}_0} + O(p^2), \tag{22}$$

where $\langle\tau\rangle_{\boldsymbol{x}_0}$ is the mean FPT to the target for a single particle started from $\boldsymbol{x}_0$. Similarly, $\widetilde{H}(p) = 1 - p\langle\tau\rangle + O(p^2)$, where $\langle\tau\rangle$ is the mean rebinding time,

$$\langle\tau\rangle = \frac{1}{|\Gamma|}\int_\Gamma d\boldsymbol{x}_0\, \langle\tau\rangle_{\boldsymbol{x}_0}. \tag{23}$$

As a consequence, Eq. (18) implies that

$$P_\infty = \frac{1}{1 + k_{\rm off}\langle\tau\rangle}. \tag{24}$$

The mean rebinding time $\langle\tau\rangle$ can be found explicitly by writing the boundary value problem for the mean FPT,

$$\begin{cases} D\Delta\langle\tau\rangle_{\boldsymbol{x}_0} &= -1 & (\boldsymbol{x}_0 \in \Omega), \\ -D\partial_n\langle\tau\rangle_{\boldsymbol{x}_0} &= \kappa \mathbf{1}_\Gamma(\boldsymbol{x}_0)\langle\tau\rangle_{\boldsymbol{x}_0} & (\boldsymbol{x}_0 \in \partial\Omega), \end{cases} \tag{25}$$

where $\mathbf{1}_\Gamma(\boldsymbol{x}_0)$ is the indicator function of Γ: $\mathbf{1}_\Gamma(\boldsymbol{x}_0) = 1$ if $\boldsymbol{x}_0 \in \Gamma$ and 0 otherwise. Integrating the first relation over $\boldsymbol{x}_0 \in \Omega$ and applying Green's formula, one gets

$$-|\Omega| = \int_\Omega d\boldsymbol{x}_0\, D\Delta\langle\tau\rangle_{\boldsymbol{x}_0} = \int_{\partial\Omega} d\boldsymbol{x}_0\, D\partial_n\langle\tau\rangle_{\boldsymbol{x}_0}$$
$$= -\int_\Gamma d\boldsymbol{x}_0\, \kappa\langle\tau\rangle_{\boldsymbol{x}_0} = -\kappa|\Gamma|\langle\tau\rangle,$$

from which

$$\langle \tau \rangle = \frac{|\Omega|}{\kappa |\Gamma|}, \tag{26}$$

where $|\Omega|$ is the volume of the domain. For a spherical target of radius ρ, the reactivity can be expressed in terms of the forward constant $k_{\rm on} = \kappa(4\pi\rho^2 N_A)$ (with $N_A \approx 6.02 \cdot 10^{23}$ mol^{-1} being the Avogadro number)[1,62] so that the mean rebinding time also reads as $\langle \tau \rangle = N_A|\Omega|/k_{\rm on}$. Defining the dimensionless quantity

$$\eta = k_{\rm off}\langle \tau \rangle = \frac{k_{\rm off}|\Omega|}{\kappa|\Gamma|} = \frac{k_{\rm off}|\Omega|N_A}{k_{\rm on}}, \tag{27}$$

we simply get $P_\infty = 1/(1+\eta)$.

In general, the poles are not necessarily simple. In particular, if the unbinding rate $k_{\rm off}$ is such that $\widetilde{H}(-k_{\rm off}) = 0$, then $-k_{\rm off}$ is the pole of $\widetilde{P}(p|\boldsymbol{x}_0)$ of higher order than 1. For instance, if $-k_{\rm off}$ is the pole of order 2, the corresponding term in the spectral expansion (21) is of the form $te^{-k_{\rm off}t}$. As the set of zeros of the function $\widetilde{H}(p)$ is discrete, we will ignore such specific values of the unbinding rate $k_{\rm off}$.

Introducing

$$\widetilde{P}(p) = \frac{1}{|\Gamma|}\int_\Gamma d\boldsymbol{x}_0\, \widetilde{P}(p|\boldsymbol{x}_0) = \widetilde{H}(p)\,\widetilde{Q}(p), \tag{28}$$

we can express $\widetilde{Q}(p)$ from Eq. (16) as

$$\widetilde{Q}(p) = \frac{1}{p+k_{\rm off}} + \frac{k_{\rm off}}{p+k_{\rm off}}\widetilde{P}(p), \tag{29}$$

which in the time domain reads

$$Q(t) = e^{-k_{\rm off}t} + k_{\rm off}\int_0^t dt'\, e^{-k_{\rm off}t'}\, P(t-t'). \tag{30}$$

This relation implies that $Q(t)$ monotonously decreases from $Q(0) = 1$ to $Q(\infty) = P_\infty$ (see Appendix A 4). Substituting Eq. (21) into this relation, we get

$$Q(t) = P_\infty + Q_0 e^{-k_{\rm off}t} + \sum_{n=1}^\infty q_n e^{p_n t}, \tag{31}$$

where

$$Q_0 = 1 - P_\infty - \sum_{n=1}^\infty q_n,$$
$$q_n = \frac{v_n}{1 + p_n/k_{\rm off}} \quad (n = 1, 2, \ldots),$$
$$v_n = \frac{1}{|\Gamma|}\int_\Gamma d\boldsymbol{x}_0 v_n(\boldsymbol{x}_0),$$

and we assumed that $-k_{\rm off}$ is not the pole. On the one hand, evaluating $\widetilde{P}(p)$ at $p = -k_{\rm off}$, one finds

$$\widetilde{P}(-k_{\rm off}) = \frac{P_\infty}{-k_{\rm off}} - \sum_{n=1}^\infty \frac{v_n}{k_{\rm off}+p_n}.$$

On the other hand, Eq. (18) implies

$$\widetilde{P}(-k_{\rm off}) = \frac{\widetilde{H}(-k_{\rm off})}{-k_{\rm off} + k_{\rm off}(1-\widetilde{H}(-k_{\rm off}))} = -\frac{1}{k_{\rm off}},$$

yielding $Q_0 \equiv 0$, and thus,

$$Q(t) = P_\infty + \sum_{n=1}^\infty q_n e^{p_n t}. \tag{32}$$

In summary, Eqs. (15), (21), and (32) fully determine the exact form of the probability density $H_N(t|\boldsymbol{x}_0)$ in terms of the first-passage time statistics $H(t|\boldsymbol{x}_0)$ of a single particle. Even if $H(t|\boldsymbol{x}_0)$ is known explicitly (see an example in Appendix B), a numerical implementation of this exact solution remains challenging because it involves the following: finding zeros $\{p_n\}$ of Eq. (20), evaluation of the residues at these poles, computation of spectral expansions (21) and (32), and finally the inverse Laplace transform in Eq. (15). The practical details of this computation are discussed in Appendix C. At the same time, our exact solution opens a way to investigate the asymptotic behavior of the exact probability density $H_N(t|\boldsymbol{x}_0)$ in a rather general setting. Before turning to this analysis, we discuss the mean reaction time.

D. Mean reaction time

Relation (15) allows one to access the moments of the reaction time,

$$\langle \mathcal{T}_N^k \rangle = (-1)^k \lim_{p\to 0}\frac{\partial^k}{\partial p^k}\,\frac{\mathcal{L}\{[P(t|\boldsymbol{x}_0)]^N\}}{\mathcal{L}\{[Q(t)]^N\}}. \tag{33}$$

In particular, the mean reaction time is

$$\langle \mathcal{T}_N \rangle = \lim_{p\to 0}\left(\frac{\mathcal{L}\{t[P(t|\boldsymbol{x}_0)]^N\}}{\mathcal{L}\{[Q(t)]^N\}} - \frac{\mathcal{L}\{[P(t|\boldsymbol{x}_0)]^N\}\,\mathcal{L}\{t[Q(t)]^N\}}{(\mathcal{L}\{[Q(t)]^N\})^2}\right).$$

As both $P(t|\boldsymbol{x}_0)$ and $Q(t)$ tend to P_∞ in the long-time limit, setting $p = 0$ in the above Laplace transforms would yield divergence. To overcome this issue, one can add and subtract the term P_∞^N to each Laplace transform, e.g.,

$$\mathcal{L}\{t[P(t|\boldsymbol{x}_0)]^N\} = \int_0^\infty dt\, t\, e^{-pt}\left([P(t|\boldsymbol{x}_0)]^N - P_\infty^N + P_\infty^N\right)$$
$$= P_\infty^N/p^2 + a_1 + o(1) \qquad (p\to 0),$$

where

$$a_k = \int_0^\infty dt\, t^k\left([P(t|\boldsymbol{x}_0)]^N - P_\infty^N\right). \tag{34}$$

Introducing also

$$b_k = \int_0^\infty dt\, t^k\left([Q(t)]^N - P_\infty^N\right), \tag{35}$$

we compute the above limit as

$$\langle \mathcal{T}_N \rangle = \frac{b_0 - a_0}{P_\infty^N} = \int_0^\infty dt\,\frac{[Q(t)]^N - [P(t|\boldsymbol{x}_0)]^N}{P_\infty^N}. \tag{36}$$

Higher-order moments of $\mathcal{T}_N$ can be expressed in a similar way. For $N = 1$, this relation implies that $\langle \mathcal{T}_1 \rangle = \langle \tau \rangle_{\boldsymbol{x}_0}$, as expected. Equation (36) is a generalization of the expression for the mean slowest FPT governed by the probability density in Eq. (3),

$$\langle \mathcal{T}^{\theta}_{N,N} \rangle = \int_0^\infty dt \big(1 - [1 - S(t)]^N\big). \tag{37}$$

In fact, if there is no unbinding ($k_{\text{off}} = 0$), one gets $Q(t) = 1$, $P_\infty = 1$, and $P(t|\boldsymbol{x}_0) = 1 - S(t|\boldsymbol{x}_0)$. In Appendix A 1, we derive the large-N asymptotic behavior of this mean time,

$$\langle \mathcal{T}^{\theta}_{N,N} \rangle \propto \langle \tau \rangle \ln N \qquad (N \to \infty). \tag{38}$$

The unbinding mechanism drastically changes this asymptotic behavior into

$$\langle \mathcal{T}_N \rangle \propto \frac{(1 + k_{\text{off}} \langle \tau \rangle)^N}{k_{\text{off}} N} \qquad (N \to \infty), \tag{39}$$

i.e., a very slow logarithmic increase turns into exponential growth controlled by the unbinding rate k_{off} (see Appendix A 2). As a consequence, when many particles are needed to trigger the reaction, even a small unbinding rate can considerably alter predictions of the irreversible setting. We emphasize, however, that Eq. (39) captures only the large-N asymptotic behavior and is not applicable at small N. In particular, a non-monotonous dependence of the right-hand side of Eq. (39) on k_{off} and N is not reproduced for the mean reaction time (see further discussion in Appendix A 2).

E. Long-time behavior

The probability density $H_N(t|\boldsymbol{x}_0)$ can be formally obtained via the inverse Laplace transform in Eq. (14) by finding the poles $p_{n,N}$ of the function $\widetilde{H}_N(p|\boldsymbol{x}_0)$ in the complex plane and applying the residue theorem. This is a difficult task, even numerically, especially for large N. We focus, therefore, on the pole $p_{1,N}$ with the smallest absolute value that determines the decay time $T_N = 1/|p_{1,N}|$ of the probability density at long times,

$$H_N(t|\boldsymbol{x}_0) \propto e^{-t/T_N} \qquad (t \to \infty). \tag{40}$$

As $P(t|\boldsymbol{x}_0)$ admits the spectral decomposition (21) with the poles p_n, the poles of the numerator $\mathcal{L}\{[P(t|\boldsymbol{x}_0)]^N\}$ of Eq. (14) are obtained as all linear combinations of the form $p_{n_1} + p_{n_2} + \cdots + p_{n_N}$. In particular, the pole with the smallest absolute value is still p_1 (apart from the pole at 0). The situation is more difficult for the denominator $\mathcal{L}\{[Q(t)]^N\}$, for which we are looking not for its poles, but for zeros. Let us search for a zero of this function,

$$\mathcal{L}\{[Q(t)]^N\}(p) = \sum_{n_1=0}^{\infty} \cdots \sum_{n_N=0}^{\infty} \frac{q_{n_1} \cdots q_{n_N}}{p - p_{n_1} - \cdots - p_{n_N}}, \tag{41}$$

where we included the pole at 0 by setting $p_0 = 0$ and $q_0 = P_\infty$. As $p \to 0$, the leading term of this expression is q_0^N/p, which can be separated from the other terms. In the leading-order approximation, one can set $p = 0$ in the remaining terms,

$$0 = \mathcal{L}\{[Q(t)]^N\}(p_{1,N}) \approx \frac{q_0^N}{p_{1,N}} - \sum_{\substack{n_1=0,\ldots \\ \ldots,n_N=0, \\ n_1+\cdots+n_N>0}}^{\infty} \frac{q_{n_1} \cdots q_{n_N}}{p_{n_1} + \cdots + p_{n_N}}. \tag{42}$$

The multiple sum, from which the term with $n_1 = n_2 = \ldots = n_N = 0$ was subtracted, can be expressed in terms of an integral, yielding an approximation for the pole $p_{1,N}$,

$$p_{1,N} \approx -P_\infty^N \left(\int_0^\infty dt \big([Q(t)]^N - P_\infty^N \big) \right)^{-1}. \tag{43}$$

As a consequence, the decay rate is

$$T_N \approx P_\infty^{-N} \int_0^\infty dt \big([Q(t)]^N - P_\infty^N \big). \tag{44}$$

Curiously, this expression is very similar to expression (36) for the mean reaction time.

The accuracy of this approximation depends on various parameters such as k_{off} and N. In fact, in order to get the sum in Eq. (42), we neglected $p_{1,N}$ under the assumption that $|p_{1,N}|$ is much smaller than $|p_1|$. As N increases, the reaction event occurs at longer times, i.e., the decay time increases, and the approximation gets more accurate. In turn, the case $N = 1$ is the worst for this approximation (see discussion in Appendix A 3). Similarly, as k_{off} increases, the particles unbind more often and the decay time increases, yielding a more accurate approximation. Note that approximation (43) can be improved by accounting perturbatively for next-order corrections.

F. Short-time behavior

At short times, the main contribution to the probability density of the first-passage time comes from the particles that follow almost "direct trajectories" to the target.[27,33,44] As a consequence, the short-time behavior is generally given as

$$H(t|\boldsymbol{x}_0) \approx C_{\boldsymbol{x}_0}\, t^\alpha\, e^{-\delta^2/(4Dt)} \qquad (t \to 0), \tag{45}$$

where δ is the distance between the starting point $\boldsymbol{x}_0$ and the target region Γ, t^α is a power law correction, and $C_{\boldsymbol{x}_0}$ is the prefactor depending on the starting point, the shape of the domain, and the reactivity κ. Note that δ is either the Euclidean distance (i.e., the length of the shortest interval connecting $\boldsymbol{x}_0$ and Γ) or the geodesic distance along the shortest curvilinear path from $\boldsymbol{x}_0$ and Γ that bypasses eventual obstacles. As a rigorous derivation of this relation is beyond the scope of this paper, we use it as an assumption, under which the following results are valid (see an example in Appendix B 3).

When the starting point $\boldsymbol{x}_0$ lies on the target, $\delta = 0$ and Eq. (45) implies $H(t) \approx Ct^\alpha$ with $C = (1/|\Gamma|)\int_\Gamma d\boldsymbol{x}_0\, C_{\boldsymbol{x}_0}$, from which $\widetilde{H}(p) \approx C\Gamma(\alpha+1)p^{-1-\alpha}$ as $p \to \infty$. If $\alpha > -2$, the leading term in the denominator of Eq. (18) is p that implies for any $\boldsymbol{x}_0$,

$$\widetilde{P}(p|\boldsymbol{x}_0) \approx \frac{\widetilde{H}(p|\boldsymbol{x}_0)}{p}, \tag{46}$$

which in the time domain gives

$$P(t|\boldsymbol{x}_0) \approx \int_0^t dt'\, H(t'|\boldsymbol{x}_0) = 1 - S(t|\boldsymbol{x}_0). \tag{47}$$

When $\boldsymbol{x}_0 \notin \Gamma$, the integral of Eq. (45) yields in the lowest order

$$P(t|\boldsymbol{x}_0) \approx \frac{4DC_{\boldsymbol{x}_0}}{\delta^2}\, t^{\alpha+2}\, e^{-\delta^2/(4Dt)}, \tag{48}$$

from which Eq. (11) implies

$$\mathcal{P}_t(N|0) \approx \left(\frac{4DC_{\boldsymbol{x}_0}}{\delta^2}\right)^N t^{N(\alpha+2)}\, e^{-N\delta^2/(4Dt)}. \tag{49}$$

At short times, one has $Q(t) \approx 1$, and thus, $\mathcal{P}_t(N|N) \approx 1$ so that

$$\widetilde{H}_N(p|\boldsymbol{x}_0) \approx p\mathcal{L}\{\mathcal{P}_t(N|0)\}, \tag{50}$$

which, in turn, gives us the short-time behavior

$$H_N(t|\boldsymbol{x}_0) \approx \frac{\partial \mathcal{P}_t(N|0)}{\partial t} \approx \frac{N\delta^2}{4D}\left(\frac{4DC_{\boldsymbol{x}_0}}{\delta^2}\right)^N t^{N(\alpha+2)-2}\, e^{-N\delta^2/(4Dt)}. \tag{51}$$

This leading-order asymptotic relation can be improved by computing the next-order term in the integral of Eq. (45) that yields the correction $O(t)$ to Eq. (51), which is still independent of the unbinding rate $k_{\rm off}$. In turn, $k_{\rm off}$ appears in the correction $O(t^2)$ by using $Q(t) \approx 1 - k_{\rm off}t$ instead of $Q(t) \approx 1$ in the above derivation. The integral of this expression yields, in the leading order, the following:

$$S_N(t|\boldsymbol{x}_0) \approx 1 - \left(\frac{4DC_{\boldsymbol{x}_0}}{\delta^2}\right)^N t^{N(\alpha+2)}\, e^{-N\delta^2/(4Dt)}. \tag{52}$$

It is easy to see that for $N = 1$, the leading term of the short-time behavior in Eq. (45) is recovered. We note that the short-time behavior of the reaction time density $H_N(t|\boldsymbol{x}_0)$ is identical to that of the probability density $H^0_{N,N}(t)$ of the first-passage time $\mathcal{T}^0_{N,N}$. This result is independent of the unbinding rate $k_{\rm off}$ because the probability of an unbinding event is small at times $t \ll k_{\rm off}^{-1}$. As a consequence, for any K, one can approximate the short-time behavior of $\mathcal{T}_{K,N}$ by that of $\mathcal{T}^0_{K,N}$, for which the probability density is given explicitly by Eq. (3). Substituting here the short-time asymptotic relations (45), (47), and (48), we then get

$$\begin{aligned} H_{K,N}(t) &\approx H^0_{K,N}(t) \\ &\approx \binom{N}{K}\frac{K\delta^2}{4D}\left(\frac{4DC_{\boldsymbol{x}_0}}{\delta^2}\right)^K t^{K(\alpha+2)-2}\, e^{-K\delta^2/(4Dt)}, \end{aligned} \tag{53}$$

which generalizes Eq. (51).

III. DISCUSSION

In order to illustrate our general results, we consider a relevant example of restricted diffusion inside a reflecting sphere of radius R toward a partially reactive spherical target of radius ρ located at the origin. This geometrical setting is a simplified model of passive diffusion inside the cytoplasm toward the nucleus. It was also employed to model diffusion of calcium ions inside a presynaptic bouton toward a calcium-sensing protein.[52] The distribution of the first-passage time of a single particle was investigated in Ref. 33. In the presence of unbinding events, the exact spectral decompositions for both probabilities $P(t|\boldsymbol{x}_0)$ and $Q(t)$ were derived in Ref. 52. Appendix B summarizes former results needed for studying the problem of impatient particles.

The numerical method for evaluating the probability density $H_N(t|\boldsymbol{x}_0)$ in Eq. (15) is described in Appendix C. To validate the accuracy of this exact solution, we also performed Monte Carlo simulations, as described in Appendix D. In the following, we set $\rho = 1$ and $D = 1$ to fix the units of length and time. The radius of outer reflecting sphere is set as $R = 10$ so that the target is relatively small. All the particles start from a fixed point $\boldsymbol{x}_0$ such that either $|\boldsymbol{x}_0| = 5$ (relatively far from the target) or $|\boldsymbol{x}_0| = 2$ (relatively close to the target). To analyze the effect of unbinding events, we fix the reactivity $\kappa = 1$ (and thus the forward constant $k_{\rm on}$) and vary the unbinding rate $k_{\rm off}$. For $\kappa = 1$, the mean rebinding time $\langle\tau\rangle$ in Eq. (26) is equal to 333. Setting $k_{\rm off} = 0.003$ or $k_{\rm off} = 0.03$, we can thus examine two settings of moderate ($\eta = 1$) and strong ($\eta = 10$) unbinding kinetics, respectively. We will compare our exact solution in Eq. (15) with Monte Carlo simulations, the LMA, the irreversible binding solution, and the short-time asymptotic relation.

TABLE I. Mean reaction time $\langle\mathcal{T}_N\rangle$ and the decay time T_N for restricted diffusion toward a spherical target of radius $\rho = 1$ and reactivity $\kappa = 1$, surrounded by a reflecting concentric sphere of radius $R = 10$, for N particles started from $|\boldsymbol{x}_0| = 5$ with $D = 1$ (see Appendix B for details). Monte Carlo (MC) values of $\langle\mathcal{T}_N\rangle$ were estimated from 10^6 realizations (see Appendix D); its theoretical values were obtained by numerical integration of Eq. (36), while LMA values were given by Eq. (7). Theoretical values of the decay time T_N were estimated by fitting $S_N(t|\boldsymbol{x}_0)/H_N(t|\boldsymbol{x}_0)$ over a selected range of times; approximate values were obtained by numerical integration of Eq. (44), while the LMA values were deduced from the inverse of the smallest eigenvalue of the matrix $-W^{(N)}$. Note that all times here should be multiplied by 10^3.

		Mean $\langle\mathcal{T}_N\rangle(\times10^3)$			Decay time $T_N(\times10^3)$		
N	$k_{\rm off}$	Theory	MC	LMA	Theory	Approx.	LMA
2	0.003	1.20	1.21	1.47	1.04	0.76	1.33
	0.03	3.90	3.94	6.45	3.87	3.83	6.42
3	0.003	2.01	2.03	3.08	1.71	1.46	2.83
	0.03	27.9	28.3	81.3	28.0	27.8	81.3

Table I shows the mean reaction time for $N = 2$ and $N = 3$ with two unbinding rates $k_{\rm off}$, showing an excellent agreement between Eq. (36) and Monte Carlo simulations. In turn, the LMA overestimates the mean reaction time, the largest deviation corresponding to stronger unbinding rate $k_{\rm off}$ and larger N. In addition, Table I shows the decay time in the same setting. Expectedly, our approximation (44) is least accurate for $N = 2$ and the small unbinding rate $k_{\rm off} = 0.003$ (see Sec. II E). At $N = 3$, the agreement is better. Moreover, for faster unbinding with $k_{\rm off} = 0.03$, approximation (44) is in excellent agreement with the exact values for both $N = 2$ and $N = 3$. In contrast, the LMA predictions are much less accurate.

A. Comparison with irreversible binding case

First, we note that the limit of irreversible binding can be achieved by setting either $k_{\rm off} = 0$ or $\kappa = \infty$. In fact, in the latter case, any particle that unbinds from the target immediately rebinds and thus never leaves the target. As a consequence, the natural parameter characterizing the unbinding kinetics is the dimensionless quantity η defined by Eq. (27). When η is small, unbinding kinetics is usually considered as irrelevant. In the following, we consider the irreversible binding limit by keeping κ fixed and setting $k_{\rm off} \to 0$.

For irreversible binding, the short-time behavior of the probability density $H_{K,N}(t|\boldsymbol{x}_0)$ is given by Eq. (53). In turn, the long-time behavior follows from the spectral expansion of the probability density $H(t|\boldsymbol{x}_0)$ of the first-passage time. In fact, as restricted diffusion occurs in a bounded domain, the governing Laplace operator, $-\Delta$, has a discrete spectrum, i.e., a countable set of eigenvalues $0 < \lambda_1 \le \lambda_2 \le \lambda_3 \le \ldots \nearrow \infty$ that are associated with $L_2(\Omega)$-normalized eigenfunctions $\{u_n(\boldsymbol{x})\}$ forming a complete orthonormal basis in $L_2(\Omega)$.[74] As a consequence, the survival probability admits the standard spectral decomposition[75]

$$S(t|\boldsymbol{x}_0) = \sum_{n=1}^{\infty} c_n\, u_n(\boldsymbol{x}_0) e^{-Dt\lambda_n}, \quad c_n = \int\limits_{\Omega} d\boldsymbol{x}\, u_n(\boldsymbol{x}), \tag{54}$$

from which Eq. (3) implies

$$H^0_{N,N}(t|\boldsymbol{x}_0) \approx N D\lambda_1\, c_1 u_1(\boldsymbol{x}_0) e^{-Dt\lambda_1}. \tag{55}$$

When the target is small, one has

$$\lambda_1 \approx \frac{\kappa|\Gamma|}{D|\Omega|} = \frac{1}{D\langle\tau\rangle}, \tag{56}$$

where we used Eq. (26) for the mean rebinding time. Therefore, we get

$$H^0_{N,N}(t|\boldsymbol{x}_0) \propto e^{-t/\langle\tau\rangle} \qquad (t \to \infty). \tag{57}$$

One sees that the decay time here, $\langle\tau\rangle$, does not depend on N, in sharp contrast to the exponential growth of T_N in Eq. (44) for reversible binding.

Lawley found that the mean of the FPT $\mathcal{T}^0_{K,N}$ was determined for any *fixed* K as[47]

$$\langle\mathcal{T}^0_{K,N}\rangle \approx \frac{C}{\ln N} \qquad (N \to \infty), \tag{58}$$

with some constant C and higher-order corrections $1/(\ln N)^2$ depending on K. However, this behavior cannot be applied to $K = N$. In Appendix A 1, we show that

$$\langle\mathcal{T}^0_{N,N}\rangle \approx C' \ln N \qquad (N \to \infty), \tag{59}$$

with another constant C' determined by the decay time of the survival probability for a single particle. Even though the mean arrival time of the slowest particle differs by a factor $(\ln N)^2$ from that of the fastest particle, the need for N particles to trigger the reaction event does not considerably slow down the irreversible reaction kinetics. This observation is totally different in the case of reversible binding, for which the mean reaction time $\langle\mathcal{T}_N\rangle$ in Eq. (39) exhibits an exponential growth with N.

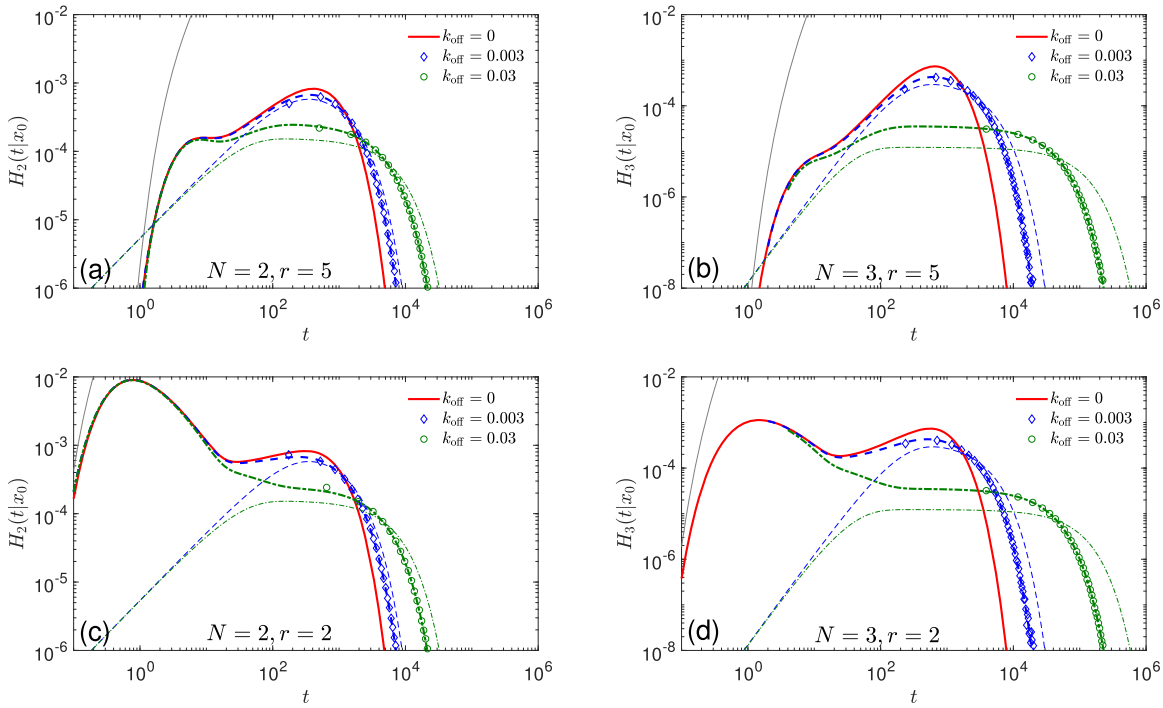

FIG. 2. Probability density $H_N(t|\boldsymbol{x}_0)$ of the reaction time $\mathcal{T}_N$ for restricted diffusion between concentric spheres of radii $\rho = 1$ and $R = 10$ with $D = 1$, $\kappa = 1$, three values of $k_{\rm off}$ (see the legend), two starting positions $|\boldsymbol{x}_0| = 5$ [(a) and (b)] and $|\boldsymbol{x}_0| = 2$ [(c) and (d)], and two values of N: $N = 2$ [(a) and (c)] and $N = 3$ [(b) and (d)]. Symbols show empirical histograms from Monte Carlo simulations with 10^6 particles. Thick lines indicate our exact solution (15) evaluated numerically as described in Appendix C, whereas thin lines show the Lawley–Madrid approximation (6). The thin gray solid line represents the short-time asymptotic behavior (51).

B. Comparison with the LMA

Now, we compare our exact results to the Lawley–Madrid approximation. This approximation was designed under assumption that the rebinding time distribution can be approximated by an exponential law: $S(t) \approx \overline{S}(t) = e^{-\nu t}$, with an appropriate rate ν. There are two natural choices for this rate. In order to get the correct long-time behavior of the survival probability, one can set $\nu = D\lambda_1$ to match the leading term of the exact spectral expansion (54). Alternatively, as the rebinding time τ is approximated by an exponential law, one can set $\nu = 1/\langle\tau\rangle$. When the target is small and weakly reactive, Eq. (56) indicates that $1/\langle\tau\rangle$ is close to $D\lambda_1$, and both choices yield the same result. One sees that the approximate equality $1/\langle\tau\rangle \approx D\lambda_1$ ensures the self-consistence of the Lawley–Madrid approximation and can thus serve as a practical indicator of its validity. As a consequence, the LMA is expected to capture the long-time behavior of the probability density $H_N(t|\boldsymbol{x}_0)$ in the limit of small targets. In the remaining part of this section, we assume that the validity conditions of the LMA are fulfilled and set $\nu = 1/\langle\tau\rangle$.

First, we look at the mean reaction time. Lawley and Madrid analyzed the asymptotic behavior of their Eq. (7) in two limits: (i) when K is fixed and $N \to \infty$, in which case $\langle\overline{\mathcal{T}}_{K,N}\rangle \sim \langle\tau\rangle K/N$, i.e., essentially a linear growth with K; (ii) when $1/(1 + k_{\text{off}}\langle\tau\rangle) < K/N < 1$ is fixed, in which case $\langle\overline{\mathcal{T}}_{K,N}\rangle$ exhibits a very rapid growth.[54] While the limiting case $K = N$ was not discussed, we deduced the asymptotic behavior of Eq. (7) by using similar tools,

$$\langle\overline{\mathcal{T}}_{N,N}\rangle \approx \frac{(1 + k_{\text{off}}\langle\tau\rangle)^N}{k_{\text{off}}N} \quad (N \gg 1). \tag{60}$$

This expression coincides with Eq. (39) that we obtained from the exact solution (36). This highlights that the LMA qualitatively captures the long-time behavior. In turn, as discussed earlier and illustrated in Table I, both Eq. (7) and its asymptotic form (60) overestimate the mean reaction time.

Let us now turn to approximation (6) of the probability density. Denoting by $0 > \nu_1 \geq \cdots \geq \nu_N$ the negative eigenvalues of the matrix $W^{(N)}$, one sees that the long-time asymptotic behavior is determined by the largest eigenvalue ν_1,

$$\overline{H}_{N,N}(t) \propto e^{-t/\overline{T}_N} \qquad (t \to \infty), \tag{61}$$

with $\overline{T}_N = -1/\nu_1$. In turn, the short-time approximation reads

$$\overline{H}_{N,N}(t) \approx \frac{N}{\langle\tau\rangle}\,(t/\langle\tau\rangle)^{N-1} + O(t^N) \quad (t \to 0), \tag{62}$$

where the lower-order powers of t vanish because of the three-diagonal structure of the matrix $W^{(N)}$, whereas the prefactor in front of the leading term t^{N-1} is $\frac{[(W^{(N)})^{N-1}]_{N,1}}{(N-1)!} = N/\langle\tau\rangle^{N-1}$. Expectedly, this asymptotic behavior is different from relation (51) derived

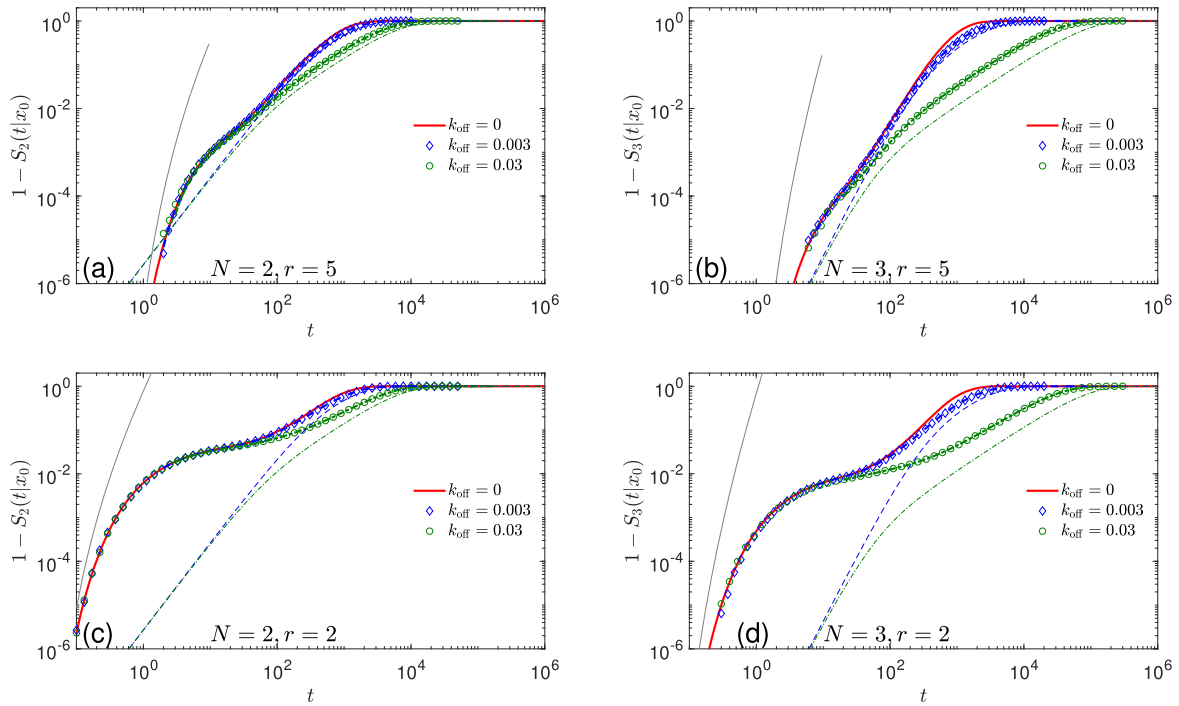

FIG. 3. Cumulative distribution function $\mathbb{P}\{\mathcal{T}_N < t\} = 1 - S_N(t|\boldsymbol{x}_0)$ of the reaction time $\mathcal{T}_N$ for restricted diffusion between concentric spheres of radii $\rho = 1$ and $R = 10$ with $D = 1$, $\kappa = 1$, three values of k_{off} (see the legend), two starting positions $|\boldsymbol{x}_0| = 5$ [(a) and (b)] and $|\boldsymbol{x}_0| = 2$ [(c) and (d)], and two values of N: $N = 2$ [(a) and (c)] and $N = 3$ [(b) and (d)]. Symbols show the empirical cumulative distribution function from Monte Carlo simulations with 10^6 particles. Thick lines indicate the integral of our exact solution (15) evaluated numerically, as described in Appendix C, whereas thin lines show the Lawley–Madrid approximation (5). The thin gray solid line represents the short-time asymptotic behavior (52).

from our exact solution. Note that in the limit $k_{\rm off} \to 0$, the assumed exponential law for the rebinding time implies

$$\lim_{k_{\rm off}\to 0} \overline{H}_{N,N}(t) = \frac{N}{\langle\tau\rangle} e^{-t/\langle\tau\rangle} \left(1 - e^{-t/\langle\tau\rangle}\right)^{N-1}. \tag{63}$$

Figure 2 illustrates the behavior of the probability density $H_N(t|\boldsymbol{x}_0)$ for two values $N = 2$ and $N = 3$ and two starting positions $|\boldsymbol{x}_0| = 5$ and $|\boldsymbol{x}_0| = 2$. First of all, we note that the probability density is broad, spanning over 4–6 orders of magnitude in time. At short times, the probability density $H_N(t|\boldsymbol{x}_0)$ does not depend on the unbinding rate $k_{\rm off}$, yielding the universal behavior of the left tail of the distribution given by Eq. (3). Note that the short-time asymptotic relation (51) is not accurate on the considered range of times but captures correctly the leading-order term. This relation can be improved by including next-order corrections. At the timescale $1/k_{\rm off}$, the unbinding mechanism starts to play a role, yielding deviations from the irreversible binding case. These deviations are actually visible already at $t \gtrsim 5$ for $k_{\rm off} = 0.03$ and $t \gtrsim 50$ for $k_{\rm off} = 0.003$. As unbinding events slow down the reaction, the right tail of the distribution is shifted toward longer times as $k_{\rm off}$ increases. In fact, the long-time decay (40) is determined by the exponential function with the decay time T_N increasing with $k_{\rm off}$. Note that Monte Carlo simulations are in perfect agreement with the exact solution.

The comparison with the LMA reveals its advantages and limitations. The LMA correctly captures the behavior of the probability density for moderate and long times, the agreement being better as $k_{\rm off}$ is smaller. One sees that the LMA systematically overestimates the decay time that controls the long-time behavior (see Table I). Deviations become larger as N and $k_{\rm off}$ increase. Expectedly, the LMA totally fails at short times. Deviations are stronger when the particles start closer to the target. In fact, when $|\boldsymbol{x}_0| = 2$, there is a notable maximum around $t \sim 1$ that is not captured by the LMA. The most probable time determining the position of this maximum is several orders of magnitude smaller than the mean reaction time. This maximum can be relevant for applications when the source of particles is close to the target (see Ref. 52 for further discussions). Nevertheless, the explicit character of the Lawley–Madrid approximation and a much simpler computation of the probability density via Eq. (6) make it a valuable tool for a first-step analysis of reversible reactions with multiple particles. Further improvements of the LMA present an important perspective.

Figure 3 represents a complementary view onto the behavior of the reaction time $\mathcal{T}_N$ by showing its cumulative distribution function $1 - S_N(t|\boldsymbol{x}_0)$.

IV. CONCLUSIONS AND PERSPECTIVES

Diffusion-controlled reactions involving multiple particles are abundant and particularly relevant in biochemistry. The need for a sufficient number of bound particles can be considered as a sort of protection mechanism against spontaneous triggering, as well as a mean for reliable control of reactions. The overwhelming majority of former studies in this field were focused on first-passage times of a single particle, with a straightforward extension to the extreme statistics of many particles with irreversible binding to the target. In turn, the problem of impatient particles with reversible binding seems to remain unnoticed, despite its practical relevance.[53] For instance, five calcium ions have to bind to a calcium-sensing protein to initiate the release of neurotransmitters for signaling between neurons.[52,55–59] To outline the role of unbinding kinetics onto this process, we take the following estimates from Ref. 52: $R = 300$ nm, $k_{\rm on} = 6.35 \cdot 10^8$ M^{-1} s^{-1} $= 6.35 \cdot 10^5$ mol m^{-3} s^{-1}, and $k_{\rm off} = 1.57 \cdot 10^4$ s^{-1}, from which the mean rebinding time is $\langle\tau\rangle \approx 0.1$ s; see Eqs. (26) and (27). As a consequence, $\eta = k_{\rm off}\langle\tau\rangle \approx 1.57 \cdot 10^3 \gg 1$ so that one cannot simply ignore reversible binding that drastically changes the distribution of the reaction time.

Even if the particles diffuse independently, their randomly "asynchronized" waiting times on the target render the problem of exact characterization of the reaction times $\mathcal{T}_{K,N}$ mathematically challenging. The remarkable work by Lawley and Madrid brought an elegant approximate solution to this problem.[54] The good accuracy of this approximation, as reported by its authors, might seem to suggest that this challenging problem is fully solved. In this paper, we showed that this is far from being the end of the story.

We focused on the particular case of the first time $\mathcal{T}_N = \mathcal{T}_{N,N}$ when all N particles are bound to the target. This choice allowed us to derive, for the first time, the exact complete solution of the problem of impatient particles, i.e., to express the probability density of the random variable $\mathcal{T}_N$ in terms of the first-passage time distribution of a single particle. This exact solution revealed some limitations and deficiencies of the LMA. In particular, we showed that the approximate solution captures the qualitative behavior at moderate and long times but fails at short times. Moreover, the LMA overestimates the mean reaction time and the decay time so that its predictions are inaccurate in some settings. At the same time, the complexity of the exact solution for $\mathcal{T}_{N,N}$ and yet a fully open problem of finding the exact solution in the general case $\mathcal{T}_{K,N}$ make the LMA a valuable tool for the qualitative analysis and preliminary estimations. Moreover, the accuracy of the LMA is expected to be much higher in the limit of very small targets. We believe that further improvements of the LMA or development of alternative methods can bring important insights on the problem of impatient particles. This is an interesting perspective of the present work.

We also emphasize that impatient particles offer an excellent example of a physical problem, for which standard numerical methods may be insufficient for getting the whole picture. In particular, as the mean reaction time and the decay time grow exponentially fast with the number of particles, getting the whole distribution of the reaction time $\mathcal{T}_N$ was not possible even for moderate N. For instance, a Monte Carlo simulation with 10^6 realizations used to plot the empirical probability density in Fig. 2 took one day on a laptop. However, this simulation allowed us to get the behavior of $H_N(t|\boldsymbol{x}_0)$ only for a limited range of time scales (e.g., from 10^2 to 10^4 for $N = 2$). Even though parallelization can easily increase the number of realizations (say by a factor 100 or 1000), it would not be enough to get the short-time behavior. As the computational time explodes with N, we could not complete Monte Carlo simulations even for moderate values of N such as $N = 5$ or $N = 10$. Here, analytical tools and approximations are indispensable.

While we focused on the setting when all particles start from the same fixed point $\boldsymbol{x}_0$, our exact solution can be easily extended to a more general case with distinct starting points. Moreover, the

starting point of each particle can also be random. In the case of a uniform distribution of the starting points, the properties of the fastest FPT $\mathcal{T}^0_{1,N}$ were studied in Ref. 48. An extension to the reaction time $\mathcal{T}_N$ is straightforward.

The exact expression (36) for the mean reaction time $\langle \mathcal{T}_N \rangle$ opens a way to investigate the role of different parameters onto the reaction kinetics. A rough approximation allowed us to access the large-N asymptotic behavior of this quantity. However, the asymptotic formula (39) lacks an exact prefactor and also fails at small N. More accurate analysis of Eq. (36) could hopefully improve this formula to get a quantitatively accurate description of the mean reaction time. Its extension to other reaction times $\langle \mathcal{T}_{K,N} \rangle$ presents an exciting perspective.

ACKNOWLEDGMENTS

D.S.G. acknowledges the Alexander von Humboldt Foundation for support within a Bessel Prize award. A.K. was supported by the Prime Minister's Research Fellowship (PMRF) of the Government of India.

AUTHOR DECLARATIONS

Conflict of Interest

The authors have no conflicts of interest to disclose.

DATA AVAILABILITY

The data that support the findings of this study are available from the corresponding author upon reasonable request.

APPENDIX A: MATHEMATICAL DETAILS

In this appendix, we discuss some asymptotic relations and derivations.

1. Mean reaction time for irreversible binding

The mean fastest FPT $\mathcal{T}^0_{1,N}$ and, more generally, the mean Kth fastest FPT $\mathcal{T}^0_{K,N}$ were thoroughly investigated in the irreversible binding case.[43–47] For any fixed K, the mean value $\langle \mathcal{T}^0_{K,N} \rangle$ behaves universally as $1/\ln N$ in the large N limit, whereas the higher-order corrections $O[1/(\ln N)^2]$ depend on K. In turn, the asymptotic behavior of the slowest FPT $\mathcal{T}^\theta_{N,N}$ was not discussed, to our knowledge. In particular, the former result for any fixed K cannot be applied to the case $K = N$. Here, we sketch the main steps of this analysis, more rigorous derivations being beyond the scope of this paper.

As the mean time $\langle \mathcal{T}^\theta_{N,N} \rangle$ is given by Eq. (37), its asymptotic analysis is reduced to that of the survival probability $S(t|\boldsymbol{x}_0)$ for a single particle. It is easy to check that the function $f(t) = 1 - (1 - S(t|\boldsymbol{x}_0))^N$ monotonously decreases from 1 at $t = 0$ to 0 as $t \to \infty$. The integral in Eq. (37) can be evaluated by approximating $f(t)$ by the Heaviside step function $\Theta(t_N - t)$, where t_N is chosen by setting $f(t_N) = \zeta$, with ζ being around 1/2 (see below). This equation yields $S(t_N|\boldsymbol{x}_0) = 1 - (1 - \zeta)^{1/N}$. When N is large, the right-hand side of this relation is close to 0. In other words, the limit $N \to \infty$ corresponds to large t_N, for which the spectral expansion (54) can be truncated to a single term, $S(t_N|\boldsymbol{x}_0) \approx c_1 u_1(\boldsymbol{x}_0) e^{-D\lambda_1 t_N}$. As a consequence, one gets

$$\langle \mathcal{T}^\theta_{N,N} \rangle \approx t_N \approx -\frac{\ln(1 - (1-\zeta)^{1/N}) - \ln(c_1 u_1(\boldsymbol{x}_0))}{D\lambda_1} \approx \frac{\ln N + \ln(c_1 u_1(\boldsymbol{x}_0)) - \ln\ln\frac{1}{1-\zeta}}{D\lambda_1}. \tag{A1}$$

Even though this approximate relation depends on a somewhat arbitrary choice of ζ around 1/2, this dependence is weak and corresponds to the sub-leading (constant) term, as compared to the leading term $\ln N$. Note that $1/(D\lambda_1)$ is the decay time for a single particle, which determines the natural timescale of the problem. Figure 4 illustrates the dependence of $\langle \mathcal{T}^\theta_{N,N} \rangle$ on N and its large-N asymptotic behavior (A1).

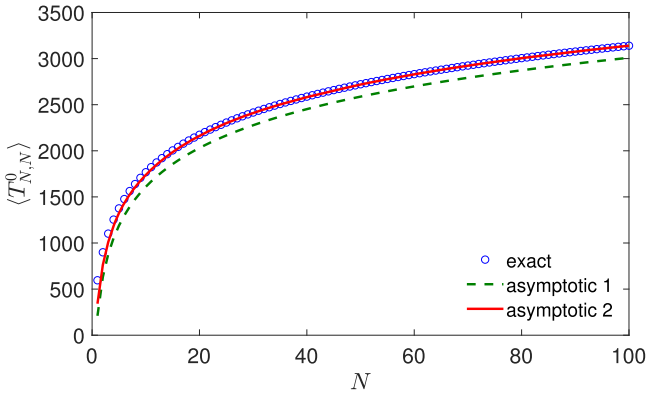

FIG. 4. Mean slowest FPT $\langle \mathcal{T}^\theta_{N,N} \rangle$ for restricted diffusion between concentric spheres of radii $\rho = 1$ and $R = 10$ with $|\boldsymbol{x}_0| = 5$, $D = 1$, $\kappa = 1$, and $k_{\text{off}} = 0$ (irreversible binding). Empty circles show the results of a numerical integration of Eq. (37), the dashed line represents Eq. (A1) with $\zeta = 0.5$, and the solid line illustrates Eq. (A1) with $\zeta = 0.428$, which was selected to get the best agreement.

2. Mean reaction time

The mean reaction time $\langle \mathcal{T}_N \rangle$ is determined by Eq. (36). We note that the function $[Q(t)]^N - [P(t|\boldsymbol{x}_0)]^N$ monotonously decreases from 1 at $t = 0$ to 0 as $t \to \infty$. We also checked that, for large N, this function decreases fast enough to allow for truncation of the integral at some finite time t_N, whereas the term $[P(t|\boldsymbol{x}_0)]^N$ is small for $t < t_N$ and can be omitted.

One can thus apply the same approximation as in Appendix A 1. In fact, we aim at evaluating t_N at which $[Q(t_N)]^N = \zeta$ or, equivalently, $Q(t_N) = \zeta^{1/N}$, with some ζ around 1/2. As $\zeta^{1/N}$ is close to 1, one considers the short-time approximation, for which $Q(t) = 1 - k_{\text{off}} t + O(t^2)$ [see Eq. (30) and Appendix A 4]. We thus get $t_N = (1 - \zeta^{1/N})/k_{\text{off}} \approx \ln(1/\zeta)/(N k_{\text{off}})$ as $N \to \infty$, from which

$$\langle \mathcal{T}_N \rangle \approx \frac{(1 + k_{\text{off}}\langle \tau \rangle)^N \ln(1/\zeta)}{k_{\text{off}} N} \qquad (N \to \infty), \tag{A2}$$

where we used Eq. (24). We stress that the prefactor $\ln(1/\zeta)$ stands here in front of the leading term, whereas in Appendix A 1, an arbitrary parameter ζ appeared only in the sub-leading term in Eq. (A1),

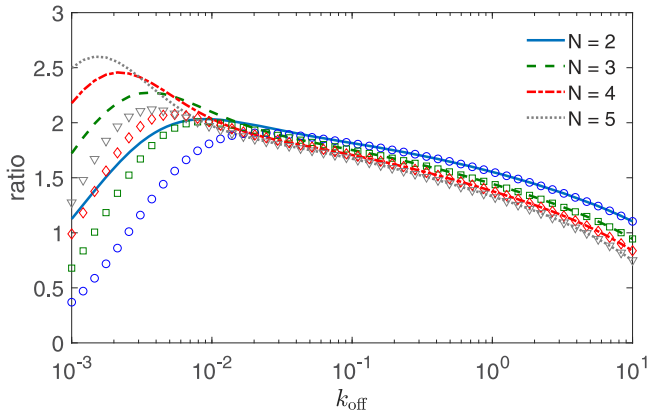

FIG. 5. The rescaled mean reaction time $\langle \mathcal{T}_N \rangle\, k_{\rm off} N P_\infty^N$ (lines) and the rescaled decay time $T_N\, k_{\rm off} N P_\infty^N$ (symbols) as functions of $k_{\rm off}$ for restricted diffusion between concentric spheres of radii $\rho = 1$ and $R = 10$ with $|\boldsymbol{x}_0| = 5$, $D = 1$, $\kappa = 1$, and $N = 2$ (circles and solid line), $N = 3$ (squares and dashed line), $N = 4$ (diamonds and dashed-dotted line), and $N = 5$ (triangles and dotted line). Theoretical values of $\langle \mathcal{T}_N \rangle$ and T_N were obtained by numerical integration of Eqs. (36) and (44), respectively.

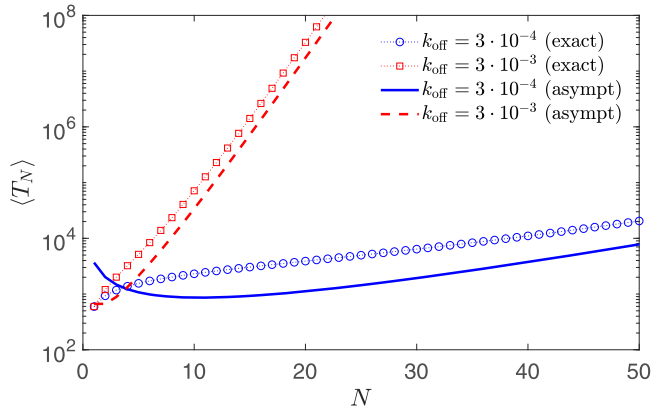

FIG. 6. Mean reaction time $\langle \mathcal{T}_N \rangle$ (symbols) and its asymptotic form (39) as functions of N for restricted diffusion between concentric spheres of radii $\rho = 1$ and $R = 10$ with $|\boldsymbol{x}_0| = 5$, $D = 1$, $\kappa = 1$, and two values of $k_{\rm off}$. Theoretical values of $\langle \mathcal{T}_N \rangle$ were obtained by numerical integration of Eq. (36).

while the leading term was universal. This feature highlights the deficiency of approximation (A2). Figure 5 compares the exact mean reaction time $\langle \mathcal{T}_N \rangle$ and the asymptotic behavior $P_\infty^{-N}/(k_{\rm off} N)$ for several values of N. While the overall behavior is correctly captured, deviations are considerable and depend on the parameters. The curves shown in Fig. 5 can be interpreted as the dependence of $\ln(1/\zeta)$ on $k_{\rm off}$ and N. Further improvements of this approximation present an interesting perspective. Note also that the asymptotic behavior (A2) with $\ln(1/\zeta) = 1$ is identical to Eq. (60) from the LMA.

In a first approximation, one may attempt to set the factor $\ln(1/\zeta)$ to 1, as in Eq. (60). The non-monotonous dependence of the right-hand side of the asymptotic form (A2) on $k_{\rm off}$ and N may suggest that the mean reaction time can be optimized with respect to these parameters. In fact, its derivative with respect to N vanishes at

$$N_c = \frac{1}{\ln(1 + k_{\rm off}\langle \tau \rangle)}, \tag{A3}$$

suggesting that $\langle \mathcal{T}_N \rangle$ can be minimized with respect to N when $k_{\rm off}\langle \tau \rangle$ is small enough. Similarly, the derivative with respect to $k_{\rm off}$ vanishes at

$$k_{\rm off,c} = \frac{1}{(N-1)\langle \tau \rangle}, \tag{A4}$$

suggesting a minimum of $\langle \mathcal{T}_N \rangle$. However, this fictitious optimality results from a rough asymptotic formula (A2) and does not occur when the exact solution (36) is considered (see Fig. 6). This example illustrates danger of relying on approximate solutions and urges for a more elaborate analysis of the exact solution.

3. The decay time for $N = 1$

As mentioned in Sec. II E, approximation (44) of the decay time T_N is least accurate in the case $N = 1$. To illustrate this point, we note that the integral in Eq. (44) can be found explicitly for $N = 1$. In fact, one has

$$\begin{aligned}
\int_0^\infty dt (Q(t) - P_\infty) &= \lim_{p\to 0}\left(\widetilde{Q}(p) - \frac{P_\infty}{p}\right) \\
&= \lim_{p\to 0}\left(\frac{1}{p + k_{\rm off}(1 - \widetilde{H}(p))} - \frac{P_\infty}{p}\right) \\
&= \lim_{p\to 0}\left(\frac{1}{p + k_{\rm off}(p\langle \tau \rangle - p^2\langle \tau^2/2 \rangle + O(p^3))} - \frac{P_\infty}{p}\right) \\
&= \frac{1}{2} P_\infty^2 k_{\rm off}\langle \tau^2 \rangle,
\end{aligned}$$

where we used Eq. (24). As a consequence, approximation (44) reads

$$p_{1,1} \approx -\frac{2}{P_\infty k_{\rm off}\langle \tau^2 \rangle}. \tag{A5}$$

Note that for restricted diffusion between concentric spheres, the second moment of the rebinding time is known explicitly; see Eq. (B6). However, a similar approximation can be used to estimate the first pole of $\widetilde{Q}(p)$ by expanding $\widetilde{H}(p)$ in Eq. (16) up to the second order in p, from which $p_1 \approx -2/(P_\infty k_{\rm off}\langle \tau^2 \rangle)$. In other words, $p_{1,1}$ turns out to be identical to p_1, thus invalidating the approximation in the case $N = 1$.

4. Behavior of the function $Q(t)$

According to Eq. (30), $Q(t)$ is a monotonously decreasing function. In fact, the time derivative of Eq. (30) reads

$$Q'(t) = -k_{\rm off}(Q(t) - P(t)). \tag{A6}$$

Comparing the probabilities $P(t)$ and $Q(t)$ of finding the particle bound to the target, one realizes that the former includes an additional step of binding to the target and thus $P(t) \le Q(t)$, implying $Q'(t) \le 0$. This property can also be deduced in a more formal way.

In fact, as $P(t)$ is the convolution of $Q(t)$ and $H(t)$ [see Eq. (28)], its integration by parts yields

$$P(t) = \int_0^t dt'\, Q(t-t')H(t') = -[Q(0)S(t) - S(0)Q(t)] + \int_0^t dt'\, Q'(t-t')S(t').$$

Since $S(0) = Q(0) = 1$, one deduces

$$Q'(t) = -k_{\rm off}\left(S(t) - \int_0^t dt'\, S(t')Q'(t-t')\right), \tag{A7}$$

where $S(t) \geq 0$ is the survival probability. Applying a sort of induction argument, one can check that the right-hand side is negative. Note also that this relation implies $Q'(0) = -k_{\rm off}$ and thus $Q(t) \approx 1 - k_{\rm off}t + O(t^2)$ as $t \to 0$.

APPENDIX B: DIFFUSION BETWEEN CONCENTRIC SPHERES

In this appendix, we summarize former results needed for evaluating the probability density of the reaction time $\mathcal{T}_N$ for the practically relevant scenario of particles diffusing in a shell-like domain $\Omega = \{\boldsymbol{x} \in \mathbb{R}^3 : \rho < |\boldsymbol{x}| < R\}$ bounded between two concentric spheres of radii ρ and R. The inner sphere is a partially reactive target with reactivity κ, whereas the outer sphere is reflecting. The rotational symmetry of the problem allows for an explicit solution by separation of variables.[3,75,76] The first-passage time distribution was discussed in Ref. 33, whereas the exact solution for the probability $P(t|\boldsymbol{x}_0)$ was given in Ref. 52.

1. First-passage time density

The probability density of the first-passage time can be found by separation of variables in a standard way (see Ref. 33 for details). The rotational symmetry implies that $H(t|\boldsymbol{x}_0)$ and other related quantities depend only on time t and the radial coordinate $r = |\boldsymbol{x}_0|$. In the Laplace domain, one has

$$\widetilde{H}(p|\boldsymbol{x}_0) = \frac{g(r)}{g(\rho) - g'(\rho)\frac{D}{\kappa}}, \tag{B1}$$

where

$$g(r) = \frac{R\sqrt{p/D}\cosh\xi - \sinh\xi}{r\sqrt{p/D}}, \tag{B2}$$

with $\xi = (R-r)\sqrt{p/D}$, and $g'(r)$ is given by

$$g'(r) = \frac{(1 - Rrp/D)\sinh\xi - \xi\cosh\xi}{r^2\sqrt{p/D}}. \tag{B3}$$

The moments of the first-passage time can be found as

$$\langle \tau^k \rangle_{\boldsymbol{x}_0} = (-1)^k \lim_{p\to 0} \frac{\partial^k \widetilde{H}(p|\boldsymbol{x}_0)}{\partial p^k}. \tag{B4}$$

Setting $|\boldsymbol{x}_0| = \rho$, one also determines the moments of the rebinding time, e.g.,

$$\langle \tau \rangle = \frac{R^3 - \rho^3}{3\kappa\rho^2} \tag{B5}$$

and

$$\langle \tau^2 \rangle = \frac{2(R^3-\rho^3)^2}{9\kappa^2\rho^4} + \frac{2(5R^6 - 9R^5\rho + 5R^3\rho^3 - \rho^6)}{45D\kappa\rho^3}. \tag{B6}$$

The inversion of the Laplace transform in Eq. (B1) by means of the residue theorem yields

$$H(t|\boldsymbol{x}_0) = \frac{D}{\rho^2}\sum_{n=1}^{\infty} \hat{\alpha}_n^2\, \hat{c}_n\, u(\hat{\alpha}_n, |\boldsymbol{x}_0|)\, e^{-Dt\hat{\alpha}_n^2/\rho^2}, \tag{B7}$$

with

$$u(\alpha, r) = \frac{\rho\sin\left(\alpha\frac{R-r}{\rho}\right) - R\alpha\cos\left(\alpha\frac{R-r}{\rho}\right)}{r},$$
$$\hat{c}_n = -\frac{2\,\mu\rho^2}{\hat{\alpha}_n}\left[(\mu R(R-\rho) + R^2 + \rho^2)\hat{\alpha}_n\sin(\hat{\alpha}_n\beta) + (R(R-\rho)\hat{\alpha}_n^2 - \mu\rho^2)\cos(\hat{\alpha}_n\beta)\right]^{-1}, \tag{B8}$$

and $\hat{\alpha}_n$ (with $n = 1, 2, \ldots$) denoting the positive solutions of the trigonometric equation

$$\tan(\alpha\beta) = \frac{\alpha(\beta + (1+\beta)\mu)}{1 + \mu + (1+\beta)\alpha^2}, \tag{B9}$$

with

$$\mu = \kappa\rho/D, \qquad \beta = (R-\rho)/\rho. \tag{B10}$$

Note that the survival probability is obtained by integrating Eq. (B7),

$$S(t|\boldsymbol{x}_0) = \sum_{n=1}^{\infty} \hat{c}_n\, u(\hat{\alpha}_n, |\boldsymbol{x}_0|)\, e^{-Dt\hat{\alpha}_n^2/\rho^2}. \tag{B11}$$

2. The occupancy probability

In turn, the spectral expansion (21) of the occupancy probability $P(t|\boldsymbol{x}_0)$ was derived in Ref. 52, with $v_n(\boldsymbol{x}_0) = c_n u(\alpha_n, |\boldsymbol{x}_0|)$, where $u(\alpha, r)$ is given by Eq. (B8), $p_n = -\alpha_n^2 D/\rho^2$, and

$$c_n = \frac{2\,\mu}{\sin(\alpha_n\beta)(\alpha_n^2 w_1 + w_2) + \alpha_n\cos(\alpha_n\beta)(\alpha_n^2 w_3 + w_4)},$$

where

$$w_1 = 4(1+\beta) + \beta(\beta + \mu(1+\beta)), \tag{B12a}$$
$$w_2 = 2(1 + \mu - \lambda(1+\beta)) - \lambda\beta^2, \tag{B12b}$$
$$w_3 = \beta(1+\beta), \tag{B12c}$$
$$w_4 = \beta(1 + \mu - \lambda(1+\beta)) - 3(\beta + \mu(1+\beta)), \tag{B12d}$$

$\lambda = k_{\rm off}\rho^2/D$, and α_n are strictly positive solutions of the trigonometric equation

$$\sin(\alpha_n\beta) = \frac{\left[\alpha_n^2(\beta + \mu(1+\beta)) - \lambda\beta\right]\alpha_n\cos(\alpha_n\beta)}{\alpha_n^4(1+\beta) + \alpha_n^2(1 + \mu - \lambda(1+\beta)) - \lambda}, \tag{B13}$$

enumerated by $n = 1, 2, \ldots$. Note that the coefficients v_n determining $Q(t)$ in Eq. (32) are simply $v_n = c_n u(\alpha_n, \rho)$.

3. Short-time asymptotic behavior

Here, we focus on the short-time behavior of $H(t|\boldsymbol{x}_0)$. As the solution in Eq. (B7) depends only on the radial coordinate $r = |\boldsymbol{x}_0|$, we replace $\boldsymbol{x}_0$ by r in the following expressions. Setting $s = (R-\rho)^2 p/D$ and $\nu = D/(\kappa\rho)$, we can rewrite $\widetilde{H}(p|r)$ as

$$\widetilde{H}(p|r) = \frac{\beta\sqrt{s}\cosh\left(\sqrt{s}\frac{R-r}{R-\rho}\right) - \sinh\left(\sqrt{s}\frac{R-r}{R-\rho}\right)}{r/\rho} \times \left((\nu+\beta)\sqrt{s}\cosh(\sqrt{s}) - (1+\nu-\gamma s)\sinh(\sqrt{s})\right)^{-1}, \tag{B14}$$

where $\gamma = \nu\beta^2\rho/R$. We first study the case $r = \rho$, for which

$$\widetilde{H}(p|\rho) = \frac{1 - \frac{1}{\beta\sqrt{s}}\tanh(\sqrt{s})}{1 + \nu/\beta - \frac{1+\nu-\gamma s}{\beta\sqrt{s}}\tanh(\sqrt{s})}. \tag{B15}$$

For large s, $\tanh(\sqrt{s}) = 1 + O(e^{-2\sqrt{s}})$, which further implies

$$\widetilde{H}(p|\rho) \approx \frac{\beta\sqrt{s} - 1}{(\nu+\beta)\sqrt{s} - (1+\nu) + \gamma s} = \frac{1}{\gamma}\left(\frac{A_1}{\sqrt{s}+x_1} + \frac{A_2}{\sqrt{s}+x_2}\right),$$

where

$$x_{1,2} = \frac{(\nu+\beta) \pm \sqrt{(\nu+\beta)^2 + 4\gamma(1+\nu)}}{2\gamma} \tag{B16}$$

and

$$A_1 = \frac{1+\beta x_1}{x_1 - x_2}, \qquad A_2 = \frac{1+\beta x_2}{x_2 - x_1}. \tag{B17}$$

Using the following inverse Laplace transform:

$$\mathcal{L}\left\{\frac{1}{\sqrt{s}+a}\right\} = \frac{1}{\sqrt{\pi\tau}} - a e^{a^2\tau}\mathrm{erfc}(a\sqrt{\tau}) = f_a(\tau) \tag{B18}$$

[where $\mathrm{erfc}(z)$ is the complementary error function], we find the short-time approximation

$$H(t|\rho) \approx D\frac{A_1 f_{x_1}\left(\frac{Dt}{(R-\rho)^2}\right) + A_2 f_{x_2}\left(\frac{Dt}{(R-\rho)^2}\right)}{(R-\rho)^2\gamma}. \tag{B19}$$

Using $f_a(\tau) \approx 1/\sqrt{\pi\tau} - a + 2a^2\sqrt{\tau/\pi} + O(\tau)$, one gets

$$H(t|\rho) \approx \frac{\kappa}{\sqrt{\pi D t}} + \kappa(1/\rho + \kappa/D) + 2\frac{\kappa(1/\rho + \kappa/D)^2}{\sqrt{\pi}}\sqrt{Dt} + O(t). \tag{B20}$$

For the case of $\rho < r < R$, we have

$$\widetilde{H}(p|r) \approx \frac{\rho}{r} e^{-\sqrt{s}(r-\rho)/(R-\rho)}\widetilde{H}(p|\rho), \tag{B21}$$

where we neglected the terms of the order $e^{-2\sqrt{s}}$ and $e^{-2\sqrt{s}\delta}$ with $\delta = (R-r)/(R-\rho)$. Note that if r is close to R (i.e., if δ is very small), the above approximation would be slightly modified. Since the Laplace transform is expressed as a product of two terms, the inverse Laplace transform yields the following convolution:

$$H(t|r) \approx \frac{\rho}{r}\int_0^t dt' H(t-t'|\rho)\frac{(r-\rho)e^{-(r-\rho)^2/(4Dt')}}{\sqrt{4\pi D t'^3}}, \tag{B22}$$

which can be evaluated using the asymptotic expression for $H(t|\rho)$ to give

$$H(t|r) = \frac{\rho\kappa e^{-(r-\rho)^2/(4Dt)}}{r\sqrt{\pi D t}}\left(1 + \frac{2Dt(1+\kappa\rho/D)}{\rho(r-\rho)} + \cdots\right). \tag{B23}$$

One can recognize Eq. (45) in the leading term, with $\alpha = -1/2$ and

$$C_{\boldsymbol{x}_0} = \frac{\rho\kappa}{r\sqrt{\pi D}}. \tag{B24}$$

APPENDIX C: NUMERICAL IMPLEMENTATION

Our central formula (15) expresses the probability density $H_N(t|\boldsymbol{x}_0)$ in terms of the accessible probabilities $P(t|\boldsymbol{x}_0)$ and $Q(t)$. However, its practical implementation requires the computation of two Laplace transforms, $\mathcal{L}\{[P(t|\boldsymbol{x}_0)]^N\}$ and $\mathcal{L}\{[Q(t)]^N\}$, and then the evaluation of the inverse Laplace transform of their ratio. Since both $P(t|\boldsymbol{x}_0)$ and $Q(t)$ are given as spectral expansions, such a computation becomes numerically difficult, especially at small and large times when $H_N(t|\boldsymbol{x}_0)$ rapidly decays. We also attempted a direct solution of the following related deconvolution problem:

$$[P(t|\boldsymbol{x}_0)]^N = \int_0^t dt' H_N(t'|\boldsymbol{x}_0)[Q(t-t')]^N, \tag{C1}$$

but it was numerically unstable.

To resolve this difficulty, one can integrate Eq. (C1) by parts to transform it into an integral equation on the survival probability $S_N(t|\boldsymbol{x}_0) = \mathbb{P}\{\mathcal{T}_N > t\}$,

$$[Q(t)]^N - [P(t|\boldsymbol{x}_0)]^N = S_N(t|\boldsymbol{x}_0) - \int_0^t dt' S_N(t'|\boldsymbol{x}_0) q_N(t-t'), \tag{C2}$$

where we used $Q(0) = S_N(0|\boldsymbol{x}_0) = 1$ and defined

$$q_N(t) = -\frac{d}{dt}[Q(t)]^N = -N[Q(t)]^{N-1}\frac{dQ}{dt}. \tag{C3}$$

Considering the last term in Eq. (C2) as the application of an integral operator $\mathcal{Q}$ to the function $S_N(t|\boldsymbol{x}_0)$, one can formally invert this relation to get

$$S_N(t|\boldsymbol{x}_0) = (I - \mathcal{Q})^{-1}\left([Q(t)]^N - [P(t|\boldsymbol{x}_0)]^N\right), \tag{C4}$$

where I is the identity operator. Expanding the operator $(I-\mathcal{Q})^{-1}$ into the geometric series, one finally expresses the survival probability as

$$S_N(t|\boldsymbol{x}_0) = \int_0^t dt'\left([Q(t')]^N - [P(t'|\boldsymbol{x}_0)]^N\right)R(t-t'), \tag{C5}$$

where

$$R(t) = (I - \mathcal{Q})^{-1}\delta(t) = \delta(t) + q_N(t) + \int_0^t dt_1\, q_N(t_1)\, q_N(t - t_1) + \cdots, \quad \text{(C6)}$$

i.e., the sum of convolutions of $q_N(t)$ with itself of all orders.

In practice, we compute both $[Q(t)]^N - [P(t|\boldsymbol{x}_0)]^N$ and $q_N(t)$ over a linear grid of points $\{0, \delta, 2\delta, \ldots, \delta(K-1)\}$ and then evaluate convolutions by fast Fourier transform (FFT). In this way, one gets the survival probability evaluated at grid points,

$$S_N(j\delta|\boldsymbol{x}_0) \approx \mathcal{F}^{-1}\left\{\frac{\mathcal{F}\{p_k\}}{1 - \mathcal{F}\{q_k\}}\right\}, \quad \text{(C7)}$$

with $j = 0, 1, \ldots, K-1$, where $p_k = c_k\left([Q(k\delta)]^N - [P(k\delta|\boldsymbol{x}_0)]^N\right)$, $q_k = \delta c_k q_N(k\delta)$, $c_0 = 1/2$, $c_k = 1$ for $0 < k < K$ and $c_k = 0$ for $K \le k < 2K$. Here, the coefficient c_0 accounts for the integration weight $1/2$ of the first point, whereas c_k for $k \ge K$ allow one to pad the vectors by 0 for the proper computation of linear convolutions via direct ($\mathcal{F}$) and inverse ($\mathcal{F}^{-1}$) FFTs applied to vectors of length $2K$. Note that the probability density $H_N(t|\boldsymbol{x}_0)$ can also be found via FFT as

$$H_N(j\delta|\boldsymbol{x}_0) \approx \frac{1}{\delta}\mathcal{F}^{-1}\left\{\left(e^{2\pi ik/(2K)} - 1\right)\frac{\mathcal{F}\{p_k\}}{1 - \mathcal{F}\{q_k\}}\right\}, \quad \text{(C8)}$$

in analogy with the evaluation of a derivative via standard Fourier transform: $f'(x) = \mathcal{F}^{-1}\{ik\mathcal{F}\{f(x)\}\}$.

The time step δ sets the minimal time at which both $S_N(t|\boldsymbol{x}_0)$ and $H_N(t|\boldsymbol{x}_0)$ are available and controls the accuracy of the whole computation. In fact, it determines how accurately discrete sums approximate convolution integrals. This is particularly important for the evaluation of $\mathcal{F}\{q_k\}$, whose maximal value is achieved at the zero frequency,

$$\max\{|\mathcal{F}\{q_k\}|\} = \mathcal{F}_0\{q_k\} = \sum_{k=0}^{2K-1} q_k \approx \int_0^{t_{\max}} dt\, q_N(t) = 1 - [Q(t_{\max})]^N \approx 1 - P_\infty^N < 1.$$

As a consequence, $1/(1 - \mathcal{F}\{q_k\})$ is well defined. However, when N or k_{off} increase, the maximum approaches to 1. If δ is not small enough, inaccurate discretization may result in $\mathcal{F}_0\{q_k\}$ exceeding 1 and thus strong instabilities in the above computation. For the computation of theoretical curves in Fig. 2, we used $\delta = 0.01$ in all cases, except for the case $k_{\text{off}} = 0.03$ and $N = 3$, for which $\delta = 0.005$ was needed.

APPENDIX D: MONTE CARLO SIMULATIONS

Monte Carlo simulations were realized via a standard event-driven scheme. Each particle was equipped by its internal "clock" t_i and the binary state variable s_i indicating whether the particle is bound or not. At time 0, all particles are free ($s_i = 1$) and released from a fixed point $\boldsymbol{x}_0$, with their clocks being set to 0. The particles diffuse independently and bind the target at random times sampled from the probability density $H(t|\boldsymbol{x}_0)$. The internal clock of each particle is thus set to its (individual) first-binding time, while their states are set to 0 (bound). We emphasize that these FPTs account for partial reactivity of the target, i.e., for eventual failed binding attempts and reflections from the target, until the successful binding. Selecting the particle with the minimal internal clock (say, t_i), one updates this clock by adding a random waiting time δ_i generated from the exponential law with the rate k_{off} and sets its state variable s_i to 1 (free). In other words, t_i is replaced by $t_i + \delta_i$, which is the instance when the ith particle unbinds from the target and resumes its diffusion. From now on, the following step is repeated: one selects the particle with the minimal internal time (say, t_j); if $s_j = 0$ (i.e., at the instance t_j the particle binds to the target), we evaluate the number of bound particles at time t_j, and the simulation is stopped if all particles are bound; if the simulation is not stopped, the clock t_j is updated by adding either a newly generated random waiting time δ_j (if $s_j = 0$) or a random rebinding time τ sampled from the probability density $H(t)$ (if $s_j = 1$). This step is repeated until the simulation is stopped (see Fig. 1).

The first-binding times are generated from the known probability density $H(t|\boldsymbol{x}_0)$ given by Eq. (B7). To sample from a broad distribution $H(t|\boldsymbol{x}_0)$ spanning several orders of magnitude in time, we first perform a change of variable $\zeta = \ln t$ and obtain the associated probability density $H_1(\zeta|\boldsymbol{x}_0)$. Prior to running simulations, we create a linear grid of possible values ζ_k, ranging from $\zeta_{\min}$ to $\zeta_{\max}$, with a step $d\zeta = 0.01$, and a grid containing the probability weight $H_1(\zeta_k|\boldsymbol{x}_0)d\zeta$ of each value ζ_k. Using these probability weights, a (pseudo)-random value of ζ is generated by using the Matlab function randsample, and the corresponding first-binding time is obtained as e^{ζ}. The same method is used for generating rebinding times from the known probability density $H(t)$.

For the considered example of restricted diffusion between two spheres, the explicit form of the survival probability $H(t|\boldsymbol{x}_0)$ is provided in Appendix B. The spectral decomposition (B11) was truncated at a large order $n = 10\,000$ in order to access accurately the short-time behavior of $H(t|\boldsymbol{x}_0)$. The zeros $\hat{\alpha}_n$ of Eq. (B9) were found by the bisection method (see Refs. 33 and 52 for details). The grid bounds $\zeta_{\min}$ and $\zeta_{\max}$ depend on the parameters and were chosen manually to cover a broad range of times whose probability density is not negligible [e.g., we used $\zeta_{\min} = -15$ and $\zeta_{\max} = 10$ for computing $H(t)$ for $\kappa = 1$].

REFERENCES

[1] D. A. Lauffenburger and J. Linderman, *Receptors: Models for Binding, Trafficking, and Signaling* (Oxford University Press, Oxford, 1993).
[2] B. Alberts *et al.*, *Molecular Biology of the Cell*, 5th ed. (Garland Science, Taylor & Francis Group, New York, 2008).
[3] S. Redner, *A Guide to First Passage Processes* (Cambridge University Press, Cambridge, 2001).
[4] Z. Schuss, *Brownian Dynamics at Boundaries and Interfaces in Physics, Chemistry, and Biology* (Springer, New York, 2013).
[5] *First-Passage Phenomena and Their Applications*, edited by R. Metzler, G. Oshanin, and S. Redner (World Scientific, Singapore, 2014).
[6] *Chemical Kinetics: Beyond The Textbook*, edited by G. Oshanin, R. Metzler, and K. Lindenberg (World Scientific, New Jersey, 2019).
[7] D. S. Grebenkov, "NMR survey of reflected Brownian motion," Rev. Mod. Phys. **79**, 1077–1137 (2007).
[8] O. Bénichou and R. Voituriez, "From first-passage times of random walks in confinement to geometry-controlled kinetics," Phys. Rep. **539**, 225–284 (2014).
[9] D. Holcman and Z. Schuss, "The narrow escape problem," SIAM Rev. **56**, 213–257 (2014).

[10]I. V. Grigoriev, Y. A. Makhnovskii, A. M. Berezhkovskii, and V. Y. Zitserman, "Kinetics of escape through a small hole," J. Chem. Phys. **116**, 9574 (2002).
[11]A. Singer, Z. Schuss, D. Holcman, and R. S. Eisenberg, "Narrow escape. Part I," J. Stat. Phys. **122**, 437–463 (2006).
[12]A. Singer, Z. Schuss, and D. Holcman, "Narrow escape. Part II. The circular disk," J. Stat. Phys. **122**, 465 (2006).
[13]A. Singer, Z. Schuss, and D. Holcman, "Narrow escape. Part III. Riemann surfaces and non-smooth domains," J. Stat. Phys. **122**, 491 (2006).
[14]S. Condamin, O. Bénichou, V. Tejedor, R. Voituriez, and J. Klafter, "First-passage time in complex scale-invariant media," Nature **450**, 77 (2007).
[15]O. Bénichou and R. Voituriez, "Narrow-escape time problem: Time needed for a particle to exit a confining domain through a small window," Phys. Rev. Lett. **100**, 168105 (2008).
[16]O. Bénichou, D. Grebenkov, P. Levitz, C. Loverdo, and R. Voituriez, "Optimal reaction time for surface-mediated diffusion," Phys. Rev. Lett. **105**, 150606 (2010).
[17]O. Bénichou, C. Chevalier, J. Klafter, B. Meyer, and R. Voituriez, "Geometry-controlled kinetics," Nat. Chem. **2**, 472–477 (2010).
[18]S. Pillay, M. J. Ward, A. Peirce, and T. Kolokolnikov, "An asymptotic analysis of the mean first passage time for narrow escape problems. Part I. Two-dimensional domains," SIAM Multiscale Model. Simul. **8**, 803–835 (2010).
[19]A. F. Cheviakov, M. J. Ward, and R. Straube, "An asymptotic analysis of the mean first passage time for narrow escape problems. Part II. The sphere," SIAM Multiscale Model. Simul. **8**, 836–870 (2010).
[20]D. S. Grebenkov, "Searching for partially reactive sites: Analytical results for spherical targets," J. Chem. Phys. **132**, 034104 (2010).
[21]A. F. Cheviakov, A. S. Reimer, and M. J. Ward, "Mathematical modeling and numerical computation of narrow escape problems," Phys. Rev. E **85**, 021131 (2012).
[22]C. Caginalp and X. Chen, "Analytical and numerical results for an escape problem," Arch. Ration. Mech. Anal. **203**, 329–342 (2012).
[23]T. G. Mattos, C. Mejía-Monasterio, R. Metzler, and G. Oshanin, "First passages in bounded domains: When is the mean first passage time meaningful," Phys. Rev. E **86**, 031143 (2012).
[24]A. M. Berezhkovsky and L. Dagdug, "Effect of binding on escape from cavity through narrow tunnel," J. Chem. Phys. **136**, 124110 (2012).
[25]J.-F. Rupprecht, O. Bénichou, D. S. Grebenkov, and R. Voituriez, "Exit time distribution in spherically symmetric two-dimensional domains," J. Stat. Phys. **158**, 192–230 (2015).
[26]A. Godec and R. Metzler, "First passage time distribution in heterogeneity controlled kinetics: Going beyond the mean first passage time," Sci. Rep. **6**, 20349 (2016).
[27]A. Godec and R. Metzler, "Universal proximity effect in target search kinetics in the few-encounter limit," Phys. Rev. X **6**, 041037 (2016).
[28]D. S. Grebenkov, "Universal formula for the mean first passage time in planar domains," Phys. Rev. Lett. **117**, 260201 (2016).
[29]J. S. Marshall, "Analytical solutions for an escape problem in a disc with an arbitrary distribution of exit holes along its boundary," J. Stat. Phys. **165**, 920–952 (2016).
[30]D. S. Grebenkov and G. Oshanin, "Diffusive escape through a narrow opening: New insights into a classic problem," Phys. Chem. Chem. Phys. **19**, 2723–2739 (2017).
[31]Y. Lanoiselée, N. Moutal, and D. S. Grebenkov, "Diffusion-limited reactions in dynamic heterogeneous media," Nat. Commun. **9**, 4398 (2018).
[32]D. S. Grebenkov, R. Metzler, and G. Oshanin, "Towards a full quantitative description of single-molecule reaction kinetics in biological cells," Phys. Chem. Chem. Phys. **20**, 16393–16401 (2018).
[33]D. S. Grebenkov, R. Metzler, and G. Oshanin, "Strong defocusing of molecular reaction times results from an interplay of geometry and reaction control," Commun. Chem. **1**, 96 (2018).
[34]V. Sposini, A. Chechkin, and R. Metzler, "First passage statistics for diffusing diffusivity," J. Phys. A: Math. Theor. **52**, 04LT01 (2019).
[35]D. S. Grebenkov, R. Metzler, and G. Oshanin, "Full distribution of first exit times in the narrow escape problem," New J. Phys. **21**, 122001 (2019).
[36]N. Levernier, M. Dolgushev, O. Bénichou, R. Voituriez, and T. Guérin, "Survival probability of stochastic processes beyond persistence exponents," Nat. Commun. **10**, 2990 (2019).
[37]D. S. Grebenkov, "Spectral theory of imperfect diffusion-controlled reactions on heterogeneous catalytic surfaces," J. Chem. Phys. **151**, 104108 (2019).
[38]D. Hartich and A. Godec, "Extreme value statistics of ergodic Markov processes from first passage times in the large deviation limit," J. Phys. A: Math. Theor. **52**, 244001 (2019).
[39]D. Hartich and A. Godec, "Interlacing relaxation and first-passage phenomena in reversible discrete and continuous space Markovian dynamics," J. Stat. Mech. **2019**, 024002.
[40]D. S. Grebenkov, "Paradigm shift in diffusion-mediated surface phenomena," Phys. Rev. Lett. **125**, 078102 (2020).
[41]D. S. Grebenkov, "Diffusion toward non-overlapping partially reactive spherical traps: Fresh insights onto classic problems," J. Chem. Phys. **152**, 244108 (2020).
[42]S. N. Majumdar, A. Pal, and G. Schehr, "Extreme value statistics of correlated random variables: A pedagogical review," Phys. Rep. **840**, 1–32 (2020).
[43]G. H. Weiss, K. E. Shuler, and K. Lindenberg, "Order statistics for first passage times in diffusion processes," J. Stat. Phys. **31**, 255–278 (1983).
[44]K. Basnayake, A. Hubl, Z. Schuss, and D. Holcman, "Extreme narrow escape: Shortest paths for the first particles among n to reach a target window," Phys. Lett. A **382**, 3449–3454 (2018).
[45]K. Basnayake, Z. Schuss, and D. Holcman, "Asymptotic formulas for extreme statistics of escape times in 1, 2 and 3-dimensions," J. Nonlinear Sci. **29**, 461–499 (2019).
[46]S. D. Lawley and J. B. Madrid, "A probabilistic approach to extreme statistics of Brownian escape times in dimensions 1, 2, and 3," J. Nonlinear Sci. **30**, 1207–1227 (2020).
[47]S. D. Lawley, "Distribution of extreme first passage times of diffusion," J. Math. Biol. **80**, 2301–2325 (2020).
[48]D. S. Grebenkov, R. Metzler, and G. Oshanin, "From single-particle stochastic kinetics to macroscopic reaction rates: Fastest first-passage time of N random walkers," New J. Phys. **22**, 103004 (2020).
[49]K. Reynaud, Z. Schuss, N. Rouach, and D. Holcman, "Why so many sperm cells," Commun. Integr. Biol. **8**, e1017156 (2015).
[50]Z. Schuss, K. Basnayake, and D. Holcman, "Redundancy principle and the role of extreme statistics in molecular and cellular biology," Phys. Life Rev. **28**, 52–79 (2019).
[51]J. B. Madrid and S. D. Lawley, "Competition between slow and fast regimes for extreme first passage times of diffusion," J. Phys. A: Math. Theor. **53**, 335002 (2020).
[52]M. Reva, D. A. DiGregorio, and D. S. Grebenkov, "A first-passage approach to diffusion-influenced reversible binding: Insights into nanoscale signaling at the presynapse," Sci. Rep. **11**, 5377 (2021).
[53]D. S. Grebenkov, "First passage times for multiple particles with reversible target-binding kinetics," J. Chem. Phys. **147**, 134112 (2017).
[54]S. D. Lawley and J. B. Madrid, "First passage time distribution of multiple impatient particles with reversible binding," J. Chem. Phys. **150**, 214113 (2019).
[55]M. J. Berridge, M. D. Bootman, and H. L. Roderick, "Calcium signalling: Dynamics, homeostasis and remodelling," Nat. Rev. Mol. Cell Biol. **4**, 517 (2003).
[56]E. Eggermann, I. Bucurenciu, S. P. Goswami, and P. Jonas, "Nanodomain coupling between Ca^{2+} channels and sensors of exocytosis at fast mammalian synapses," Nat. Rev. Neurosci. **13**, 7–21 (2012).
[57]M. Dittrich *et al.* "An excess-calcium-binding-site model predicts neurotransmitter release at the neuromuscular junction," Biophys. J. **104**, 2751–2763 (2013).
[58]Y. Nakamura *et al.*, "Nanoscale distribution of presynaptic Ca^{2+} channels and its impact on vesicular release during development," Neuron **85**, 145–158 (2015).
[59]C. Guerrier and D. Holcman, "Hybrid Markov-mass action law model for cell activation by rare binding events: Application to calcium induced vesicular release at neuronal synapses," Sci. Rep. **6**, 35506 (2016).
[60]F. C. Collins and G. E. Kimball, "Diffusion-controlled reaction rates," J. Colloid Sci. **4**, 425 (1949).

[61] H. Sano and M. Tachiya, "Partially diffusion-controlled recombination," J. Chem. Phys. **71**, 1276–1282 (1979).
[62] D. Shoup and A. Szabo, "Role of diffusion in ligand binding to macromolecules and cell-bound receptors," Biophys. J. **40**, 33 (1982).
[63] R. Zwanzig, "Diffusion-controlled ligand binding to spheres partially covered by receptors: An effective medium treatment," Proc. Natl. Acad. Sci. U. S. A. **87**, 5856 (1990).
[64] B. Sapoval, "General formulation of Laplacian transfer across irregular surfaces," Phys. Rev. Lett. **73**, 3314–3317 (1994).
[65] M. Filoche and B. Sapoval, "Can one hear the shape of an electrode? II. Theoretical study of the Laplacian transfer," Eur. Phys. J. B **9**, 755–763 (1999).
[66] O. Bénichou, M. Moreau, and G. Oshanin, "Kinetics of stochastically gated diffusion-limited reactions and geometry of random walk trajectories," Phys. Rev. E **61**, 3388–3406 (2000).
[67] D. S. Grebenkov, M. Filoche, and B. Sapoval, "Spectral properties of the Brownian self-transport operator," Eur. Phys. J. B **36**, 221–231 (2003).
[68] A. M. Berezhkovskii, Y. A. Makhnovskii, M. I. Monine, V. Y. Zitserman, and S. Y. Shvartsman, "Boundary homogenization for trapping by patchy surfaces," J. Chem. Phys. **121**, 11390 (2004).
[69] D. S. Grebenkov, "Partially reflected Brownian motion: A stochastic approach to transport phenomena," in *Focus on Probability Theory*, edited by L. R. Velle (Nova Science Publishers, 2006), pp. 135–169.
[70] D. S. Grebenkov, M. Filoche, and B. Sapoval, "Mathematical basis for a general theory of Laplacian transport towards irregular interfaces," Phys. Rev. E **73**, 021103 (2006).
[71] J. Reingruber and D. Holcman, "Gated narrow escape time for molecular signaling," Phys. Rev. Lett. **103**, 148102 (2009).
[72] S. D. Lawley and J. P. Keener, "A new derivation of Robin boundary conditions through homogenization of a stochastically switching boundary," SIAM J. Appl. Dyn. Syst. **14**, 1845–1867 (2015).
[73] A. J. Bernoff, A. E. Lindsay, and D. D. Schmidt, "Boundary homogenization and capture time distributions of semipermeable membranes with periodic patterns of reactive sites," Multiscale Model. Simul. **16**, 1411–1447 (2018).
[74] D. S. Grebenkov and B.-T. Nguyen, "Geometrical structure of Laplacian eigenfunctions," SIAM Rev. **55**, 601–667 (2013).
[75] C. W. Gardiner, *Handbook of Stochastic Methods for Physics, Chemistry and the Natural Sciences* (Springer, Berlin, 1985).
[76] H. S. Carslaw and J. C. Jaeger, *Conduction of Heat in Solids*, 2nd ed. (Oxford University Press, 1959).